Science of the Total Environment 877 (2023) 162751

Contents lists available at ScienceDirect

Science of the Total Environment

journal homepage: www.elsevier.com/locate/scitotenv

Mobilization pilot test of PCE sources in the transition zone to aquitards by combining mZVI and biostimulation with lactic acid

Diana Puigserver [a], Jofre Herrero [b], José M. Carmona [b,*]

[a] Department of Mineralogy, Petrology and Applied Geology. Faculty of Earth Sciences, University of Barcelona (UB), Water Research Institute (IdRA-UB), Serra Húnter Tenure-elegible Lecturer, C/ Martí i Franquès, s/n, E-08028 Barcelona, Spain

[b] Department of Mineralogy, Petrology and Applied Geology, Faculty of Earth Sciences, University of Barcelona (UB), Water Research Institute (IdRA-UB), C/ Martí i Franquès, s/n, E-08028 Barcelona, Spain

HIGHLIGHTS

- A new PCE pool removal strategy was developed for transition zones to bottom aquitards.
- Oxidative bacteria removed harmful metabolites from incomplete reductive biodegradation.
- mZVI abiotically degraded PCE and its metabolites to harmless acetylene.
- Coupling mZVI and biostimulation with lactate was very effective in the pool removal.

GRAPHICAL ABSTRACT

Schematic diagram of the half-cycle cell operation

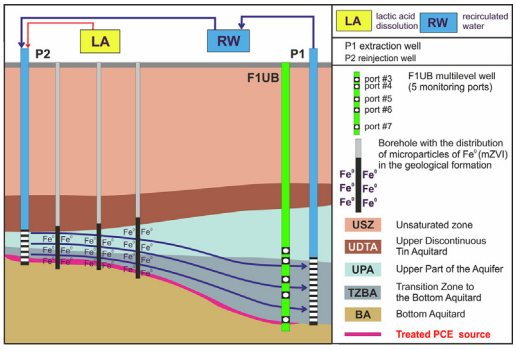

ARTICLE INFO

Editor: José Virgílio Cruz

Keywords:
PCE DNAPL pools
Remediation field pilot test
Combined remediation method
Abiotic reduction with mZVI
Biostimulation with lactate
Microbial flora in the transition zone of aquifers

ABSTRACT

The potential toxic and carcinogenic effects of chlorinated solvents in groundwater on human health and aquatic ecosystems require very effective remediation strategies of contaminated groundwater to achieve the low legal cleanup targets required. The transition zones between aquifers and bottom aquitards occur mainly in prograding alluvial fan geological contexts. Hence, they are very frequent from a hydrogeological point of view. The transition zone consists of numerous thin layers of fine to coarse-grained clastic fragments (e.g., medium sands and gravels), which alternate with fine-grained materials (clays and silts). When the transition zones are affected by DNAPL spills, free-phase pools accumulate on the less conductive layers. Owing to the low overall conductivity of this zone, the pools are very recalcitrant. Little field research has been done on transition zone remediation techniques. Injection of iron microparticles has the disadvantage of the limited accessibility of this reagent to reach the entire source of contamination. Biostimulation of indigenous microorganisms in the medium has the disadvantage that few of the microorganisms are capable of complete biodegradation to total mineralization of the parent contaminant and metabolites. A field pilot test was conducted at a site where a transition zone existed in which DNAPL pools of PCE had accumulated. In particular, the interface with the bottom aquitard was where PCE concentrations were the highest. In this pilot test, a combined strategy using ZVI in microparticles and biostimulation with lactate in the form of lactic acid was conducted. Throughout the test it was found that the interdependence of the coupled biotic and abiotic processes generated synergies between these processes. This resulted in a greater degradation of the PCE and its transformation products. With the combination of the two techniques, the mobilization of the contaminant source of PCE was extremely effective.

* Corresponding author.
E-mail addresses: puigserverdiana@ub.edu (D. Puigserver), jofreherreroferran@ub.edu (J. Herrero), jmcarmona@ub.edu (J.M. Carmona).

http://dx.doi.org/10.1016/j.scitotenv.2023.162751
Received 25 August 2022; Received in revised form 5 February 2023; Accepted 5 March 2023
Available online 13 March 2023

1. Introduction

Chloroethenes are a group of volatile organic compounds (VOCs) formed by perchloroethene (PCE), trichloroethene (TCE), cis-B85dichloroethene (cDCE), trans-dichloroethene (tDCE) and 1,1-dichloroethene (1,1-DCE) and vinyl chloride (VC). The presence of organic contaminants such as chloroethenes is common in industrial areas (Ellis and Rivett, 2007; Yu et al., 2015; Puigserver et al., 2013, 2016). Pankow and Cherry (1996) described the most significant physical and chemical properties of these products. Except for VC, their density is higher than that of water, so they are grouped within the dense non-aqueous phase liquids (DNAPLs). In addition to their density, they are characterized by other properties, notably their different sorption degrees by the particulate organic fraction of subsoil and their low rate of natural biodegradation, which represents a major constraint for the remediation of contaminated sites (Bradley, 2003). This is why they are traditionally considered to be highly recalcitrant organic compounds. In addition, they are carcinogenic, so their presence in subsurface materials and groundwater puts human health and ecosystems at risk (Hartwell, 2000; Chen et al., 2016), making their study a global challenge.

Transition zones from aquifers to bottom aquitards are mainly found in geological contexts of prograding alluvial fan deposits. These contexts are very frequent; hence the transition zones are also very common hydrogeological settings, characterized by high geological heterogeneity (Parker et al., 2003; Puigserver et al., 2013, 2020). In these zones, there are numerous textural changes where interbedded levels alternate between fine and coarse grain sizes, which result in high contrasts in hydraulic conductivity (with low and high values of this parameter, respectively). These contrasts lead to a complex architecture of the contaminant source and a slow groundwater flow rate (Luciano et al., 2012; Newell et al., 2014; Puigserver et al., 2016). Information on how free-phase DNAPL migrates and distributes in the subsurface environmental matrices can be found in the Supporting Information (SI document, Section 1.1). The complexity of the source and slow flow rate in the transition zones lead to low mass flow and account for the longevity of the contamination sources and the difficulty in mobilizing them (Parker et al., 2003; Christ et al., 2010; Brusseau et al., 2013; Rivett et al., 2014; Puigserver et al., 2013, 2016). This type of context is also characterized by numerous biogeochemical processes, a large amount of particulate and dissolved organic matter at the low hydraulic conductivity layers, and a large microbial diversity, which makes these transition zones major ecotones within the aquifer (Goldscheider et al., 2006; Puigserver et al., 2013, 2016, 2020; Griebler and Avramov, 2015). In contrast to the difficulty in mobilizing the sources, the fact that the transition zones are ecotones favors the formation of microorganism biofilms around the pools, which are capable of progressively biodegrading the pollutants that form the pools (Puigserver et al., 2016). This biologically enhanced process increases the rate of source dissolution, as observed by Yang and McCarty (2000, 2002), Puigserver et al. (2016) and Benioug et al. (2019), and can potentially be used for source mobilization.

The biotic degradation of chloroethenes occurs under different environmental conditions, although reducing conditions are predominant. The anaerobic reductive dechlorination (anaerobic respiration) is the prevalent process and the most well-studied degradation process of chloroethenes (Bradley and Chapelle, 2010; Nijenhuis and Kuntze, 2016). Traditionally this has been described as a process in which PCE is sequentially reduced to increasingly lighter metabolites, and to the harmless ethene or ethane (Hug et al., 2013; Cápiro et al., 2015; Jugder et al., 2016). However, this process is often not completed, causing the accumulation of cDCE and VC in the aquifers, thus increasing the risk to human health and ecosystems, since these are more toxic than the parent compounds from which they originate (Dolinová et al., 2017). This sequential biotic degradation has been described in different redox zones. Thus, reductive dechlorination from PCE to TCE occurs under denitrification conditions (Bradley and Chapelle, 2010; Weatherill et al., 2019), and the transformation of TCE into cDCE needs Mn- and Fe-reducing conditions (Wei and Finneran, 2011; Němeček et al., 2020). The change from cDCE to VC occurs under sulfate-reducing conditions (Amaral et al., 2011; Antoniou et al., 2019), and for degradation of VC to ethene or ethane, methanogenic conditions are needed (Aulenta et al., 2007a, 2007b; Herrero et al., 2019). In the case of prevailing conditions of a more oxic character, cDCE and VC can be oxidized (Field and Sierra-Alvarez, 2001; Findlay et al., 2016). Dolinová et al. (2017) provided an overview of the main genera of microorganisms reported by different authors to be able to degrade chloroethenes under anoxic and oxic redox conditions.

Among others, the following genera reported by Dolinová et al. (2017) can perform anaerobic respiration: *Dehalococcoides* (Rossi et al., 2012; Zinder, 2016; Saiyari et al., 2018), *Sulfurospirillum* (Buttet et al., 2013; Goris and Diekert, 2016; Gadkari et al., 2018) and *Geobacter* (Löffler et al., 2013; Cápiro et al., 2015; Němeček et al., 2017).

Oxidative biodegradation of chloroethenes is carried out by microorganisms that use these compounds as a source of carbon and energy (Němeček et al., 2020). This type of process has been detected in the presence of TCE, cDCE, and VC, the degradation of the latter compound being the most frequent (McCarty, 2016; Atashgahi et al., 2017; Baskaran and Rajamanickam, 2019). Among the genera of oxidative microorganisms listed by Dolinová et al. (2017) as capable of degrading chloroethenes are the following: *Brevundimonas* (Wilson et al., 2016), *Nocardioides* (Mattes et al., 2015; Gafni et al., 2020) and *Pseudomonas* (Schmidt et al., 2010; Bradley, 2012; Atashgahi et al., 2017). Moreover, oxidative degradation of chloroethenes has also been described as a co-metabolic degradation process by many methanotrophic bacteria that degrade toluene and phenol, including the genera *Burkholderia* (Peng and Shih, 2013; Gaza et al., 2019; Gafni et al., 2020), *Nocardioides* (Schmidt et al., 2014; Thornton et al., 2016), *Pseudomonas* (Çeçen et al., 2010; Luo et al., 2014; Yang et al., 2019), *Ralstonia* (Paszczynski et al., 2011; Li et al., 2014; Tabernacka et al., 2019), and *Variovorax* (Futamata et al., 2005; Li et al., 2014).

The coexistence in the environment of different redox processes can limit the bioavailability of electrons for microorganisms in the medium, which can inhibit the natural attenuation of these pollutants (Paul et al., 2016; Antoniou et al., 2019). An alternative solution to this electron deficit may be the supply of substrates (source of carbon) and electron donors (energy) through biostimulation, which increases the capacity of microorganisms to perform the degradation of chloroethenes (Wen et al., 2015; Zhang et al., 2016; Gupta and Widdowson, 2017).

Abiotic chemical reduction of chloroethenes has been described in natural contexts, especially in the presence of iron minerals such as pyrite (Wei et al., 2012); magnetite (Culpepper et al., 2018) and green rusts (Jeong and Hayes, 2007; Jeong et al., 2011; Fan et al., 2016; Puigserver et al., 2020, 2022). In addition, metallic iron in the form of micro- or nanoparticles, also called zero valent iron (mZVI and nZVI, respectively), has been traditionally used as a chemical reagent with significant capacity of abiotically reducing chloroethenes (Herrero et al., 2019; Phenrat et al., 2019). ZVI is a highly corrosive reagent that can generate as byproducts precipitates of neoforming minerals such as green rust (Hwang and Shin, 2013), siderite (Xie and Cwiertny, 2012), magnetite and iron oxyhydroxide (Manquián-Cerda et al., 2017), as well as iron sulfide minerals (Rajajayavel and Ghoshal, 2015) that also contribute to the abiotic degradation of chloroethenes. Among the main abiotic degradation pathways of chloroethenes the reductive elimination stands out (Schiwy et al., 2016; Berns et al., 2019), which results in the formation of dichloroacetylene (DCA) and chloroacetylene (CA) (He et al., 2015; Berns et al., 2019), which by hydrogenation can lead to the formation of ethene and/or ethane (Berns et al., 2019; Islam et al., 2020). More information on iron minerals and ZVI regarding abiotic degradation of chloroethenes and their degradation pathways can be found in the SI document (Sections 1.8, 1.9, and 1.10).

Research conducted by authors such as Tobiszewski and Namieśnik (2012) suggests that abiotic dechlorination is often slower than microbial degradation. Despite this, the interdependence of coupled abiotic and biotic processes may generate synergies between these processes, which may favor a higher rate of degradation of chlorinated solvents, including chloroethenes (Bradley and Chapelle, 2010; Puigserver et al., 2011; Patterson et al., 2016; Herrero et al., 2019; Puigserver et al., 2020; Berns et al., 2019). However, the relevance of this degradation rate depends on the abundance and nature of microorganisms in the contaminated site,

and the type of minerals involved, e.g., iron minerals in the II state (Butler et al., 2013). The confirmation of the mentioned synergies has led several authors to study at a laboratory scale the combined use of chemical reducing methods of chlorinated solvents, such as that promoted by the use of ZVI and the biostimulation of microbial flora through the addition of lactate as an electron donor (Lookman et al., 2004; Liang et al., 2007; Lorah et al., 2008; Dong et al., 2009; Puigserver et al., 2011; Patterson et al., 2016; Herrero et al., 2019). At the field level, there are some experiences in the combined use of in situ chemical reduction (ISCR) techniques and biostimulation (Lojkasek-Lima et al., 2012; Bruton et al., 2015; Wu et al., 2020), although none of them have been applied in transition zones from aquifers to aquitards in the Mediterranean climate, where large temperature and rainfall (and subsequent aquifer recharge) variations along the year affect biogeochemical processes occurring in the subsurface, which justifies the need to analyze these methodologies in the remediation of chlorinated solvents in such hydrogeological and climatic contexts.

The main objective of the present work is to analyze at the field scale the combined use of mZVI and lactate biostimulation in the form of lactic acid (LA), to favor the mobilization of the recalcitrant DNAPL sources located in the contact interfaces between the conductive and low conductive layers that constitute the transition zones between aquifers and bottom aquitards. Three working hypotheses have been proposed: i) it is possible to mobilize the recalcitrant sources of DNAPL accumulated on the numerous fine-grained and low hydraulic conductivity layers that comprise the transition zone to bottom aquitards; ii) this mobilization and subsequent degradation of dissolved PCE and transformation products is highly effective when ISCR remediation techniques are combined with the use of mZVI and lactate biostimulation; and iii) the occurrence of aerobic microorganisms ensures the products resulting from the biodegradation via incomplete reductive dechlorination of PCE can be degraded to CO_2. These hypotheses arise from the results of a microcosm experiment that the authors of the current study conducted at the laboratory scale (Herrero et al., 2019). Their results revealed the potential for replication through a pilot test at a field scale. The current study shows the main findings of this field pilot test, which demonstrate the validity of the hypotheses.

For this purpose, a site located in Vilafant, about 140 km northeast of Barcelona (Fig. 1) in an industrial area surrounded by an agricultural zone was chosen. As reported by Puigserver et al. (2016), free and residual-phase PCE pools (whose PCE mole fraction was 99.82 %) were previously detected at different depths in the unsaturated zone, in the upper part of the aquifer (UPA) and in the transition zone between the aquifer and the bottom aquitard (TZBA). According to the mentioned authors, the interface with the bottom aquitard (BA) was where PCE concentrations were the highest because of the pools accumulated. Although these pools were extremely recalcitrant due to the low hydraulic conductivity of the medium in the TZBA, incomplete biotic reductive dechlorination of PCE to TCE and cDCE was naturally occurring before the pilot test started in 2017. More information on the site can be found in the SI document (Section 2).

2. Materials and methods

2.1. Design and implementation of the pilot test remediation device

The execution of the pilot test occurred in 2017–2019 and consisted of two stages. In the first stage, six 8-m deep mZVI injection boreholes were drilled by rotation and with continuous core recovery following the

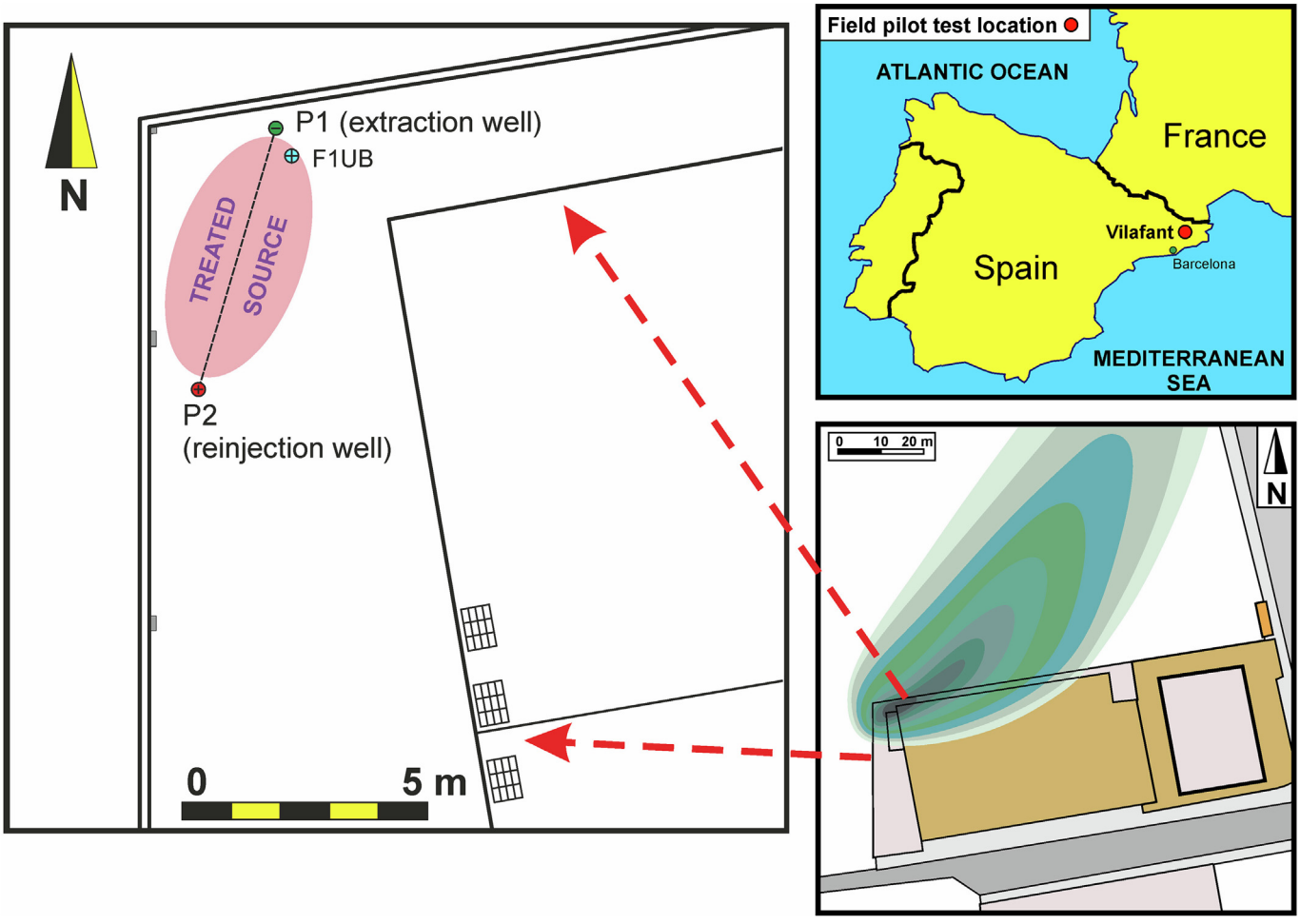

Fig. 1. Location map of the study area.

guidelines provided by Puigserver et al. (2016). The injection of an aqueous emulsion of mZVI and guar gum (both food grade quality) was carried out in the six boreholes by using groundwater from the drilled boreholes (Fig. 2A shows the location of the mZVI injection boreholes). The mZVI injection method in each borehole was hydrostatic pressure, always from bottom to top between 8 and 4.5 m depths. The total mass of mZVI injected was 30 kg (5 at each injection borehole). With the injection of the mZVI in the sixth borehole (Fig. 2A), the last one, the pilot test started. This is considered day zero of the pilot test (time 0 days).

In a second stage, a recirculation flow cell was activated on the 149th day after the start of the pilot test (time 149 days, Fig. 3A) to inject the LA solution used in the biostimulation.

The recirculation cell was conceived to biostimulate the TZBA, (Fig. 2B). Given the low hydraulic conductivity of this TZBA, the cell was designed to operate in half cycles of filling and emptying of a water recycling tank (Fig. 2B) to obtain a slow groundwater velocity within the zone of influence of the cell. A Spanish patent application has been filed by the authors of this work to the Spanish Patent and Trademark Office (SPTO).

LA was injected at 6 m depth into the reinjection well (P2), screened in the UPA, and the TZBA (Fig. 2B) throughout the pilot test on a semi-cyclical basis for nearly a year, between days 149 to 504 (355 days). The control of concentrations at P2 was not to monitor the combined strategy since it was located upgradient of the mZVI injection points. However, as only biotic degradation occurred at P2, the study of the variation of chloroethene concentrations was used to determine the biodegradation reactions of these compounds, which occurred only by biostimulation of the microbial flora. The pilot test monitoring network (Fig. 2A) consisted of a multilevel well (F1UB), and the two wells forming the cell (P1, P2). Data on the main characteristics of the monitoring points of the pilot test can be found in Table SI–1 of the SI document.

2.2. Groundwater monitoring during the pilot test

The pilot test started at the time corresponding to day 0 (first sampling day) when mZVI was injected. This reagent acted alone during the first 149 days. When this period ended (day 149), the recirculation cell was activated, and the combined treatment of mZVI and biostimulation with LA came into operation for a total of the aforementioned 355 days (i.e., until day 504). A list of groundwater sampling days from the start of the pilot test in the monitoring network can be found in Table SI–2 of the SI document.

Physicochemical parameters monitored in groundwater of the cell were dissolved oxygen (DO, mg/L), oxidation-reduction potential (ORP, mV), pH, temperature (T, °C), and electrical conductivity (EC, μS/cm). As regards concentrations of dissolved compounds, these were chloroethenes (PCE, TCE, cDCE, tDCE, 1,1-DCE, and VC), chloroacetylenes (DCA and CA), and gases (ethene, ethane, acetylene, and methane). In addition, $\delta^{13}C$ values of chloroethenes and chloroacetylenes were also determined (although in the latter case isotopic fractionation could only be determined when the concentrations were sufficiently high). Redox-sensitive species (nitrate, nitrite, Mn^{2+}, Fe^{2+}, sulfate, and sulfide), lactate, acetate, and formate were also determined. And finally, the groundwater microbial communities (phyla and genera) were identified, as well as their role in the biogeochemical processes occurring during the pilot test. The procedures and protocols followed for groundwater sampling in the monitoring network, preservation, and transport of samples, analytical techniques and laboratories are described in the SI document (Section 3.1). The processing of PCE isotopic fractionation to determine the efficiency of PCE degradation, and the processing data to identify the microorganisms occurring in the zone of influence of the cell, are also found in this document.

3. Results and discussion

3.1. Physicochemical parameters

The physicochemical conditions control the evolution of the main phyla and genera of microorganisms in the medium. Fig. 3A shows how the LA injection regime and the successive episodes of heavy rainfalls in October–November 2018 (autumn, days 400, 427, and 448) conditioned in the pilot test the most important changes in two of the physicochemical parameters that control the biogeochemical processes in the medium (ORP and DO, Fig. 3B, C).

Fig. 3 highlights how the injection of LA in P2 favored a highly reducing ORP as a consequence of the biostimulation of the microbial flora, which was accompanied by a significant decrease in DO (similar to what was observed in laboratory biostimulation microcosm experiments with LA conducted by Herrero et al. (2019) using sediments and groundwater from this site).

In the TZBA (ports F1-5UB, F1-6UB, and F1-7UB of piezometer F1UB), the injection of mZVI before cell start (on day 149, Fig. 3A) favored a decline in the ORP values in the medium (Fig. 3B), similar to what was observed by Sun et al. (2016) and Yang et al. (2018). These redox conditions were modified by the oxygenation of the medium during the first stages after cell start-up (Fig. 3A, C). Once the environmental conditions stabilized, combined action of mZVI and biostimulation with LA (Fig. 3A) again resulted in progressively lower ORP values (Fig. 3B). This trend was subsequently modified by episodes of significant rainfalls (and consequent recharge of the aquifer, Fig. 3A) that occurred during the pilot test. Thus, the accumulated rainfall between the groundwater samplings of days from 149 to 222, from 268 to 294, from 310 to 373, and from 457 to 504 (Fig. 3A) favored the input of DO, which led to oxygenation of the medium, resulting in higher ORP values (Fig. 3A, B). In contrast, the accumulated rainfall from day 373 to 457 did not modify the general trend of decreasing ORP values in the TZBA due to the increase in biostimulation with LA (Fig. 3A) of the microbial flora during that period between sampling surveys. The considerable oxygenation of the environment after day 457 due to a large amount of accumulated rainfall was noteworthy (Fig. 3A, C).

Groundwater temperature (T) ranged between 12.2 and 24.4 °C and electrical conductivity (EC) between 198 and 1926 μS/cm, with maximum EC levels recorded during the summer months. The values recorded in these parameters and their low variability throughout the pilot test allowed the favorable development of microorganism-mediated biogeochemical reactions (Kaiser and Bollag, 1990). The pH in the reinjection well (P2) tended to be acidic from late summer to late autumn (5.53 and 4.29, Fig. 3D) due to the fermentation of the injected LA (He et al., 2003), which required the injection of a buffer solution consisting of 80 % sodium bicarbonate and 20 % sodium carbonate, according to Robinson and Barry (2009). As a result of the injection of this buffer solution, downgradient of the reinjection well (P2), within the zone of influence of the cell, the pH values ranged from 7.7 to 6.8.

More data on the variability of these physicochemical parameters and redox-sensitive species (such as nitrate and nitrite; Mn^{2+}, Fe^{2+}, sulfate, and sulfide) during the pilot test in the extraction (P1) and reinjection (P2) wells and at ports F1-5UB, F1-6UB, and F1-7UB can be found in Table SI–4 of the SI document.

3.2. Phyla of identified microorganisms throughout the pilot test in P1, P2, and F1-7UB

Fig. 4 shows the evolution throughout the pilot test of the percentage of identified phyla relative to those detected. In the reinjection well (P2), phyla increased (Fig. 4A) when LA injection was initiated (Fig. 3A), although the acidification of the medium, especially from day 356 to 400, caused a slight decrease in their development. Proteobacteria was the phylum with the highest proportion within the community, and that which most increased during the pilot test (especially just after the change of the LA injection regime that started from day 294), with an increase in all classes, except δ-Proteobacteria, which remained constant. Once the cell started functioning, the microbial community at F1-7UB adapted to the new environmental conditions, closely matching the microbial community identified in P1. More information on the main phyla identified throughout the operating period of the cell can be found in the SI document (Section 4.5).

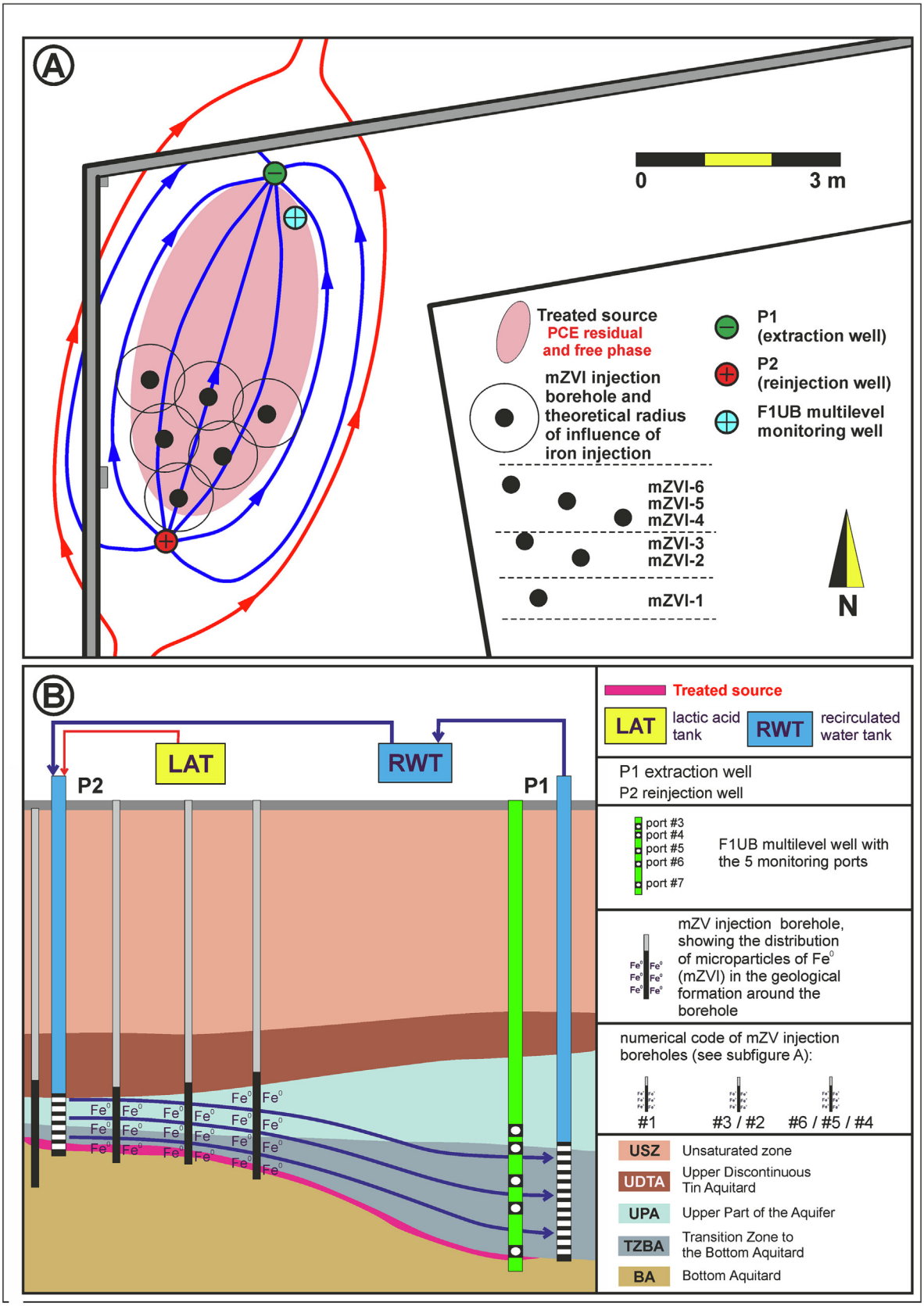

Fig. 2. (A) Zone of influence of the recirculation cell (limited by the outermost blue flow lines); location of the six injection boreholes for the mZVI and guar gum emulsion, of the extraction well (P1), of the reinjection of LA-groundwater well (P2), and of the multilevel monitoring well; (B) vertical section of the mZVI injection wells and the cell extraction-reinjection system showing the recirculating water tank and the LA stock solution tank.

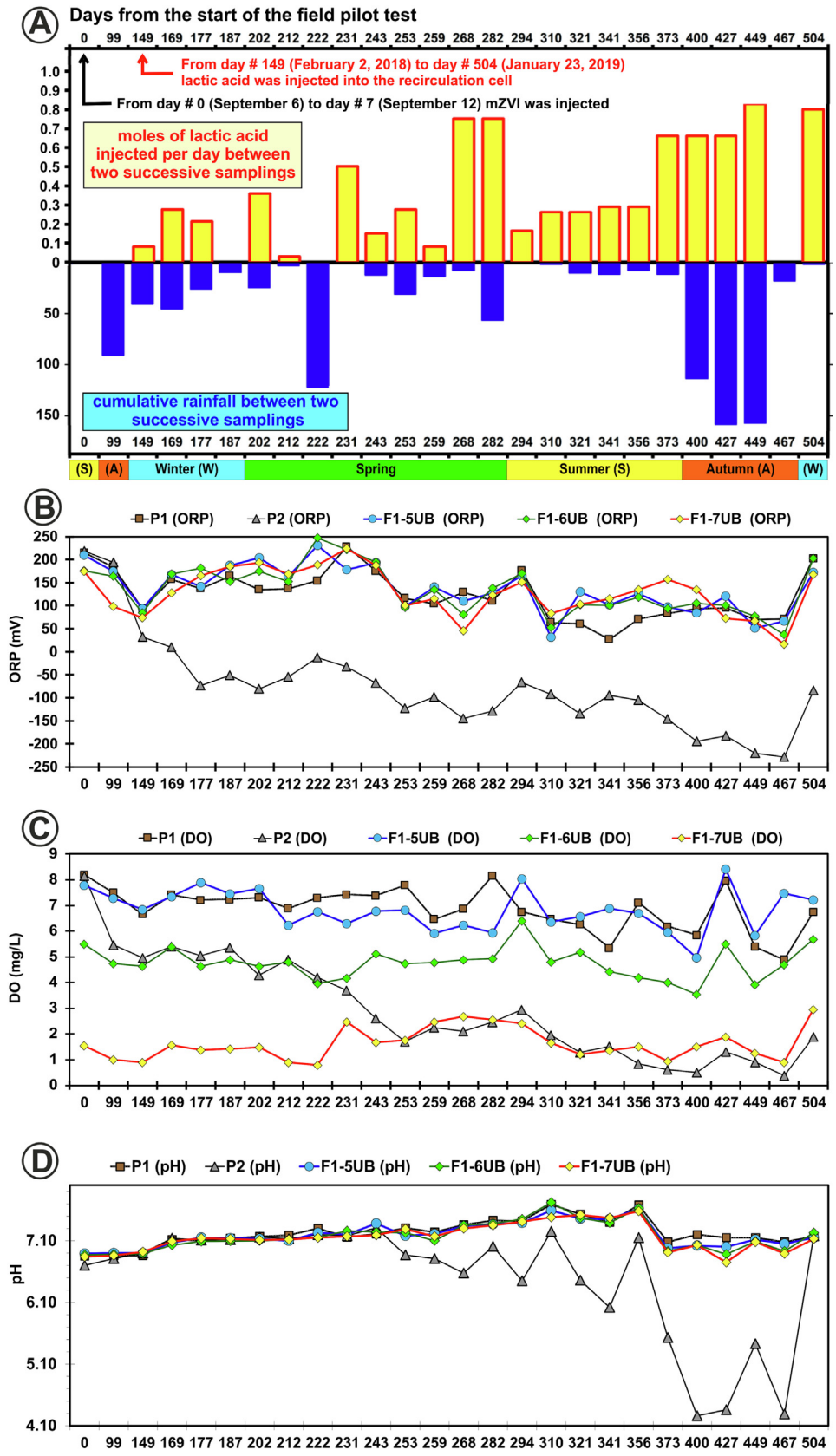

Fig. 3. (A) LA injection regime (moles/day) and cumulative rainfall (mm) between two successive survey samplings; (B), (C), and (D) evolution of ORP, DO, and pH, respectively, throughout the pilot test.

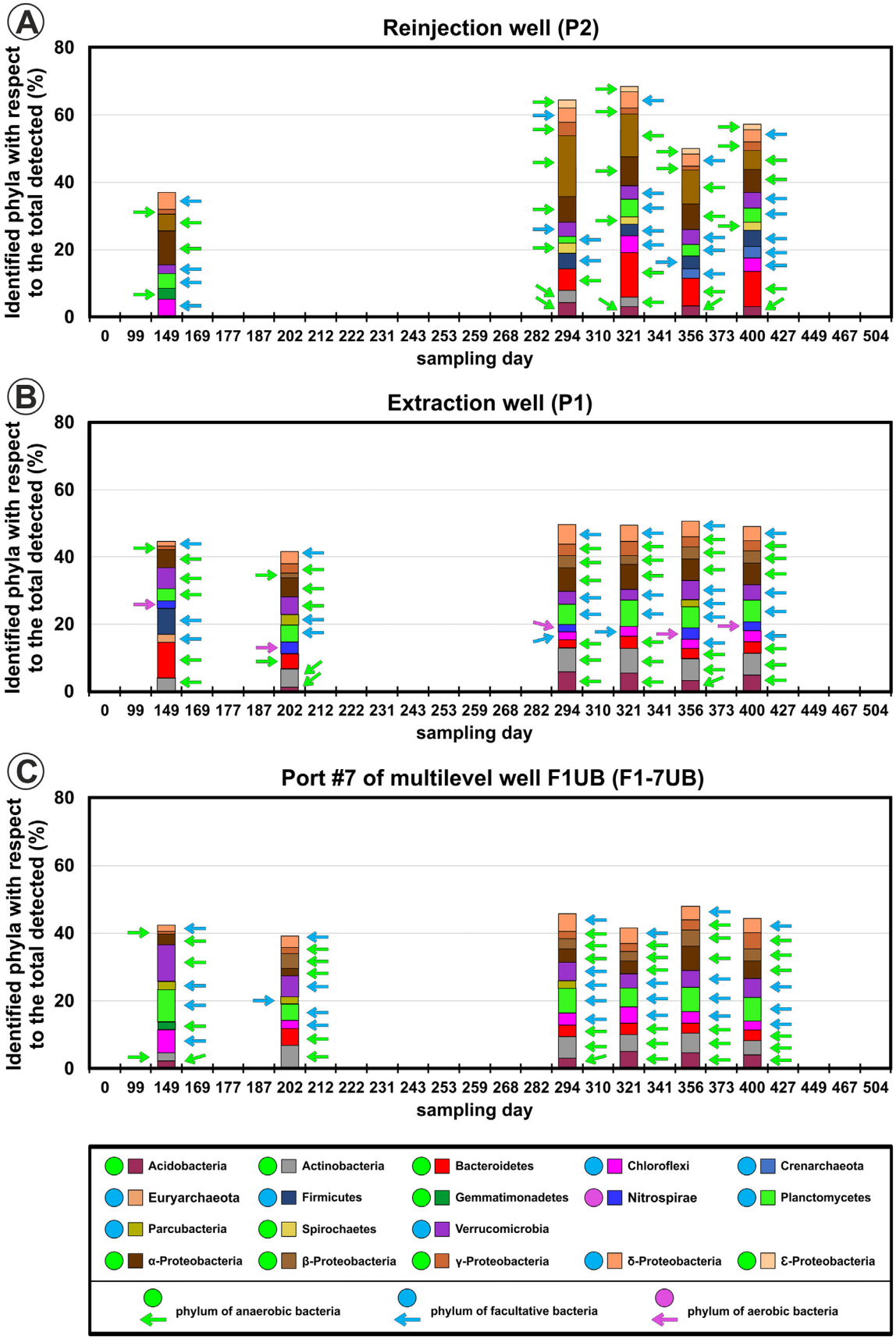

Fig. 4. Evolution of the percentage of identified phyla relative to the total number of phyla detected in groundwater during the pilot test (only phyla with a percentage higher than 2 % are shown); (A) P2 (injection well); (B) P1 (extraction well, screened in the TZBA); (C) Port F1-7UB (open at the interface between the TZBA and BA); results correspond to the following samplings: day 149 (start-up of the recycling cell), day 202 (early spring), days 294, 321, 356 (summer), and day 400 (early autumn); see Fig. 3A for variation over time of cumulative rainfall between successive sampling surveys and the LA injection regime (moles/day).

3.3. Redox-sensitive species controlling biogeochemical processes and associated microbial communities

3.3.1. Nitrate and nitrite

In general, nitrate concentrations in the zone of influence of the cell remained high because of the elevated diffuse nitrate hydrochemical background (ACA, 2019). The maximum nitrate concentrations recorded during the pilot test were 125.02 mg/L, while the minimum concentrations were 7.06 and 13.11 mg/L, at P2 and the interface between the TZBA and the BA (port F1-7UB), respectively. These minimum values derive from the fact that the LA injection well is involved in the first case, whereas the second case is because this interface is where the most reducing conditions were recorded under natural conditions (Puigserver et al., 2016). Increases in nitrate concentrations occurred as a consequence of the spreading of manure used as fertilizer in the fields, coinciding with the increase in recharge produced after the aforementioned rainfall episodes (Mohaupt et al., 2007), such as after 222 and 400 days (Fig. 3A). However, nitrate degradation was notable after these episodes, especially during the summer season. In the reinjection well (P2), LA injection resulted in highly reducing conditions, so that the decrease in nitrate concentration was very significant and sustained over time, even during periods when a substantial mass of this ion was incorporated into the medium (especially in spring, but also during the early autumn).

The decrease in nitrate was accompanied by increases in nitrite concentrations, as a consequence of the denitrification processes that occurred (Tesoriero et al., 2000), especially in P2 in the summer period, when redox conditions were highly reducing (Fig. 3B), with a decrease in nitrate concentrations from 43.76 (day 294, early summer) to 14.38 mg/L (day 373, late summer), which also allowed the existence of anaerobic ammonium oxidation processes, such as the ANAMMOX process (Cecchetti et al., 2022). Nitrite concentrations varied because of the occurrence of both oxidative and reductive processes leading to this ion (Burns et al., 1995). More information on the evolution of nitrate and nitrite concentrations throughout the pilot test can be found in Fig. SI–1 of the SI document.

3.3.2. Genera of microorganisms associated with nitrogen species

Among the genera identified as ammonium oxidizers, the presence of *Nitrospira*, belonging to the phylum Nitrospirae (Table SI–5 and SI–6 in the SI document), stands out with a higher identification percentage (Table SI–5), which indicates that under natural conditions, the process of ammonium oxidation takes place completely, which agrees with the high nitrate concentrations in the medium (Daims et al., 2015; Starke et al., 2017; Daims and Wagner, 2018). The presence of this genus in P2 decreases during the summer season due to the extremely reducing conditions in the area within the zone of influence close to the reinjection well (P2), Figs. 3B and 5.

As a result of biostimulation with LA, different ammonium oxidizing genera were detected in the TZBA after 212 days, which remained fairly constant throughout the pilot test. The presence in the summer season of the nitrifier genus *Gemmata*, which is facultative (Fig. 6A, B, C) and associated with ANAMMOX processes (Sonthiphand et al., 2014; Sekhohola-Dlamini and Tekere, 2019), stands out, following the reducing conditions of the medium in summer (Fig. 5) and with the availability of nitrite (Fig. SI–1C, D of the SI document) (Daalkhaijav and Nemati, 2014).

Of the genera identified that are nitrate reducers, the already mentioned *Nitrospira* is highlighted, which according to Koch et al. (2015) can also reduce nitrate to nitrite (in agreement with the higher nitrite concentrations in the summer season, Fig. SI–1B, C of the SI document); and the genera *Gemmatimonas* (Fig. 6) (Leigh et al., 2015; Lu et al., 2020), *Pirellula* (Liebich et al., 2009; Shirokova and Ferris, 2013; Xu et al., 2018) and *Phycisphaera* (Madigan et al., 2015). The percentages of identification of these detected genera were lower in P2 than in the TZBA (Fig. 4A), which accords with the less reducing conditions in the TZBA compared to those in P2.

In P1 (i.e. in the TZBA) during the summer season (Fig. 5), in addition to *Gemmatimona* and *Nitrospira* having been detected, increases in *Flavobacterium* and *Pirellula* were also detected, which is indicative that denitrification took place (Fedler et al., 2003; Nestler et al., 2007; Zhou et al., 2015), although no significant decrease in nitrate concentrations was detected due to the continuous input of this ion from the upgradient agricultural fields.

3.3.3. Manganous manganese and ferrous iron

A progressive increase in Mn^{2+} attributable to reduction reactions of oxidized manganese minerals (McMahon et al., 2011; Oldham et al., 2017), such as the ubiquitous pyrolusite, MnO_2, occurred during the pilot test. This was especially the case in the reinjection well (P2) and at the interface between the TZBA and the BA (at port F1-7UB). In the reinjection well P2, Mn^{2+} concentrations increased from 0.006 mg/L on day 0 (natural conditions) to 1.236 mg/L on day 356, shortly before the end of summer. In

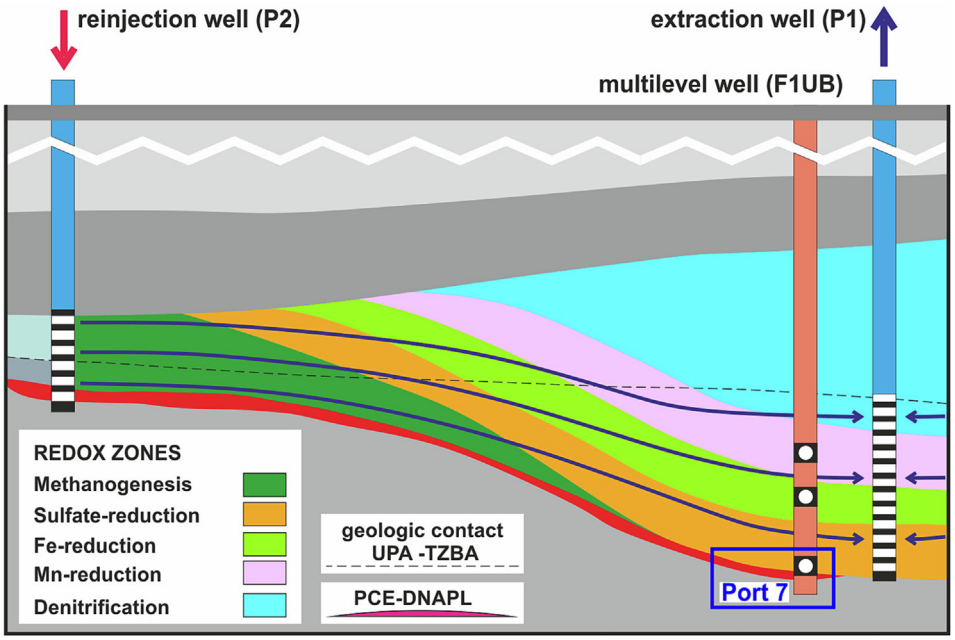

Fig. 5. Summer redox zones in the recirculation cell.

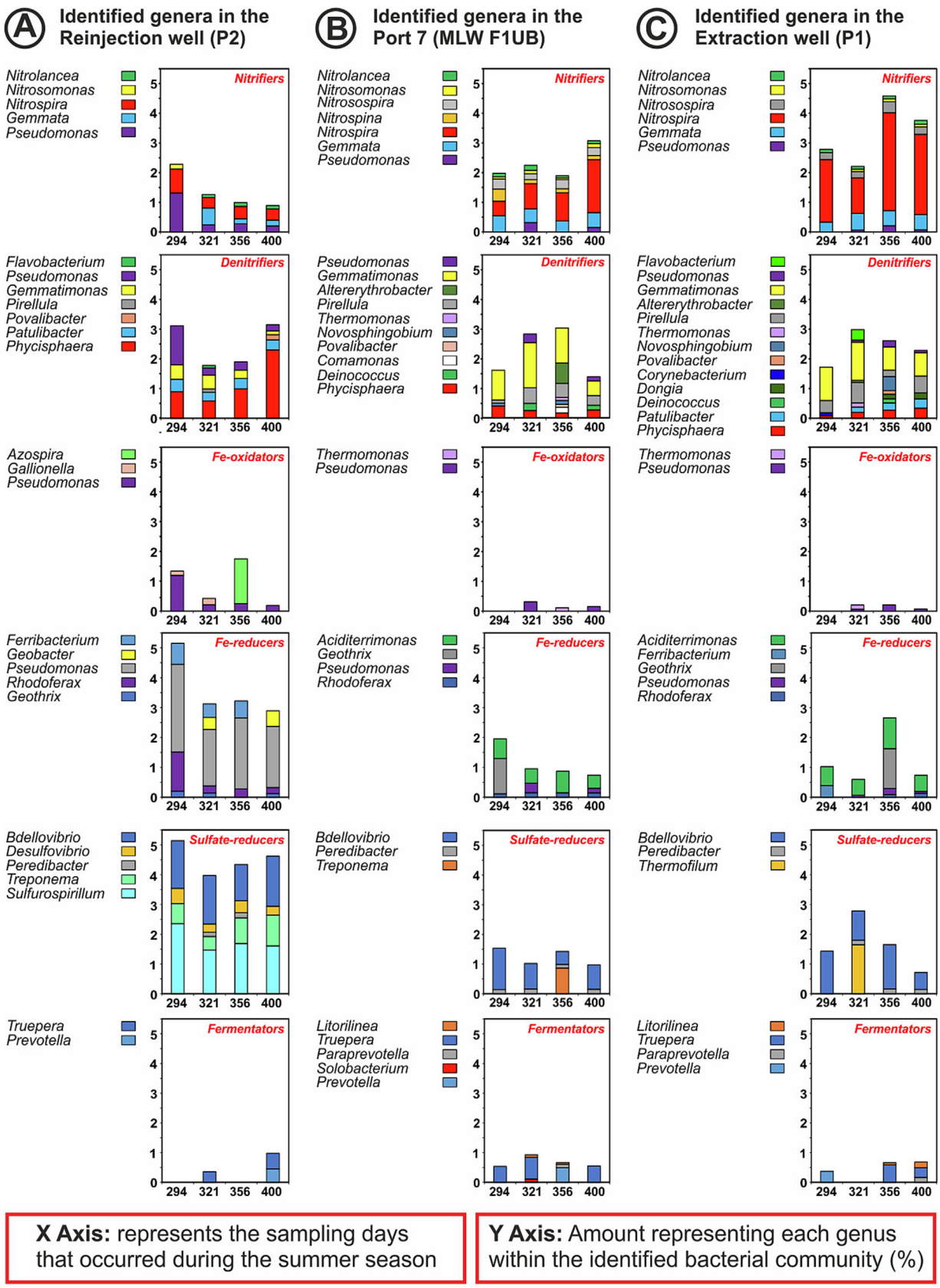

Fig. 6. Genera identified during the summer (days 294, 321, 356, and 400, Fig. 3A): nitrifiers, denitrifiers, Fe-oxidators, Fe-reducers, sulfate-reducers, and fermentators. The monitoring results for the reinjection well (P2), the F1-7UB port, and the extraction well (P1) have been selected for this figure. The port F1-7UB is located at the interface between the TZBA and the bottom aquitard and is the deepest of the multilevel monitoring well F1UB. The screened zone of the extraction well ranges from 600 to 800 mm deep (Table SI–1), hence groundwater is pumped from a depth very close to that of the F17-UB port. The numerical value assigned to each identified genus is the percentage of that genus in the detected genera of the bacterial community.

port F1-7UB, where Mn^{2+} was already detected under natural conditions, as reported by Puigserver et al. (2016), Mn^{2+} concentrations increased from 0.011 mg/L on day 0 to 0.298 mg/L on day 504 (end of the pilot test, already in winter). In contrast, in the other monitoring points, the oxygenation of the medium during rainy periods led to a lower rate of manganese reduction, which resulted in a lower mobilization of this metal from the solid to the liquid phase (Goren et al., 2012). More information on the evolution of Mn^{2+} concentrations throughout the pilot test can be found in Fig. SI–2 of the SI document.

The presence of Fe^{2+} in groundwater has essentially two origins. Part of the mobilized Fe^{2+} originated because of the oxidation process of the injected mZVI, whose oxidation resulted in an increase of electrons in the medium (Cullen et al., 2011; Stefaniuk et al., 2016). The Fe^{2+} from this oxidation process progressively decreased since the mZVI was injected. In contrast, there was an increase in this ion from sampling day 294 (early summer) until day 504 (end of the pilot test, when the maximum concentration was recorded). During this increase in Fe^{2+}, the concentration recorded in the reinjection well P2 on sampling day 294 was 0.51 mg/L, while for the rest of the sampling points (P1, F1-5UB, F1-6UB, and F1-7UB), the minimum value was 0.01 mg/L. On day 504, the concentration at P2 was 7.22 mg/L, and the maximum value among the rest of the points was 0.39 mg/L. However, the increase in Fe^{2+} described above was not a continuous process, since from sampling day 356 to day 400, a Fe^{2+} decrease occurred during a more reducing period (Fig. SI–2), which resulted in sulfate-reduction processes (Fig. SI–3) mediated by microorganisms (McMahon and Chapelle, 2008; Blöthe and Roden, 2009; Coby et al., 2011). These processes favored the precipitation of Fe^{2+} in the form of pyrite. In addition, the fact that at that time the mZVI was already in an aged state of corrosion-oxidation (so the mass of Fe^{2+} that was incorporated into the groundwater flow as a result of the oxidation of the remaining mZVI decreased, Appelo and Postma, 1996; Reinsch et al., 2010; Miao et al., 2012) also contributed to the decline of $Fe2^{+}$ in groundwater during this period. See more details in Fig. SI–2 of the SI document.

These findings confirm that, at the end of the spring, the zone of influence of the cell was within the Mn reduction redox zone, evolving towards the Fe reduction redox zone, following Christensen et al. (2000).

The maximum rate of Fe^{2+} incorporation into groundwater occurred in the reinjection well (P2) in October 2018, on sampling day 400 (Fig. SI–2C of the SI document). This was followed by a drastic decrease of this ion as a result of sulfide precipitation as pyrite, given the ORP and pH conditions recorded in the environment (Fig. 3B, D). Subsequently, the Fe^{2+} concentration recovered in P2 at the beginning of December after day 449.

3.3.4. Genera of microorganisms associated with the oxidation of iron

The presence of Fe-oxidizing genera was lower than that of reducers. Among the former (Fig. 6A), the high percentage (1.31 %) represented by the genus *Pseudomonas* (Emerson et al., 2010; Kim and Park, 2014) within the bacterial community identified is noteworthy on sampling day 294 in the reinjection well (P2, Fig. 6A). The sampling on day 294 was conducted after a period in which the injection flow rate of LA moles between two successive samplings was high, with 22 mol accumulated between successive samplings at the end of spring, between days 268 and 282, and the beginning of summer, between days 282 and 294 (Fig. 3A).

Also remarkable was the high percentage (1.64 %) of identified bacteria of the genus *Azospira* (Mattes et al., 2013) during the summer season (on day 356). The presence of this genus is indicative of anaerobic oxidation of the Fe^{2+} generated, because of the predominance of Fe-reducing conditions (Ahmed et al., 2019). Some nitrate-dependent bacteria belonging to this genus, such as *A. suillum*, capable of reducing nitrate, are associated with the precipitation of green rust (Lack et al., 2002). This mineral favors the abiotic degradation of some chlorinated solvents such as carbon tetrachloride (Puigserver et al., 2016, 2020).

In the TZBA (in the extraction well, P1) during the summer period (Fig. 3A), the presence of *Thermomonas* (on day 321, with 0.14 %) and the increase of *Pseudomonas* (from day 321 to day 356, with 0.07 % on day 321 and 0.21 % on day 356) stand out (Straub et al., 2004; Dubinina and Sorokina, 2014). These bacterial genera are responsible for the oxidation of Fe^{2+} produced as a result of the reducing conditions in the cell, which shows the synergy between the oxidation and reduction processes in the TZBA, contributing to the improvement of groundwater quality in the area of influence of the cell.

It is also noteworthy that in the F1-7UB port and P1, the percentage of Fe-oxidizing genera in the identified bacterial community was significantly lower and more constant (Fig. 6B, C) than in P2, which should be attributed to the fact that the interface zone with the bottom aquitard is being dominated by reducing conditions throughout time, so that: i) the bacterial communities are more stable and change little at the F1-7UB port and P1, and ii) the Fe^{2+} oxidation in the TZBA is only recorded at lower depths in the shallower F1UB ports, where more oxidizing conditions were present (Fig. 3A, ports F1-5UB or F1-6UB, with ORP and DO average values ranging from 34.0 to 239.0 mV, and from 4.3 to 7.4 mg/L, respectively.).

3.3.5. Genera of microorganisms associated with the reduction of iron

The highly reducing conditions in the reinjection well (P2) favored the presence of Fe-reducing genera that are strictly anaerobic (Levar et al., 2017) and chemoorganotrophic, which utilize Fe^{3+} as the main electron acceptor (Lovley, 2006). This is the case for *Geothrix* (Lonergan et al., 1996; Nevin and Lovley, 2002; Pan et al., 2017; Mehta-Kolte and Bond, 2012), with high identification percentages during the summer (sampling days 294, 321,356, and 400, Fig. 6A, average value of 2.31 %). The presence of *Pseudomonas*, *Ferribacterium* (Cummings et al., 1999), *Rhodoferax* (Baek et al., 2016), and *Geobacter* also occurred to a lesser extent.

In the TZBA, in P1, the microbial structure in some respects was similar to that recorded in P2. Thus, the maximum presence of *Geothrix* was also recorded during the summer season on day 356 (Fig. 6C, with a value of 2.31 %). However, unlike what occurred in P2, the genus *Aciditerrimonas* (Pant and Pant, 2010; Fullerton et al., 2014; Gafni et al., 2020) was observed coinciding with the Fe-reducing and sulfate-reducing conditions prevailing during the summer period in the TZBA (Fig. 5) (Itoh et al., 2011; Wei et al., 2016; Zhang et al., 2019).

In the TZBA-BA interface (port F1-7UB, Fig. 6B), from day 321, the sum of the percentages of identified *Rhodoferax*, *Pseudomonas*, and *Aciditerrimonas* progressively decreased until day 400 (from 0.95 % to 0.74 %, on days 321 and 400, respectively), which is consistent with the gradual decrease of DO in the medium that reached a minimum during the summer months (Fig. 3B, 0.93 mg/L). The decrease in these genera, in parallel with the decrease in DO, is due to the displacement of such microbial communities by others of a more reductive character, such as those of sulfate-reducing genera.

In this interface, the increase in the percentage of identified Fe-reducing genera was recorded in *Geothrix* earlier than in P1 (coinciding with the first maximum registered in P2, Fig. 6A), while the rest of the percentages of identified genera remained constant, although with a tendency to increase throughout the pilot test. Thus, more stable conditions close to iron reduction were present in this deeper zone of the TZBA (Fig. 5).

3.3.6. Sulfate and sulfide

Similarly to nitrate, the sulfate hydrochemical background was also high, although it presented a lower concentration in the TZBA than in the UPA because a portion of the sulfate was related to diffuse agricultural contamination (Puigserver et al., 2016). Throughout the pilot test, a progressive decrease in sulfate was detected, at first associated with the injection of mZVI (Fig. SI–3 of the SI document), which promoted sulfate-reduction (Hu et al., 2011; Kumar et al., 2015; Dong et al., 2019) and was accompanied by the formation of sulfide ion (S^{2-}).

In addition, during cell operation between days 231 and 373, sulfate decreased because of sulfate-reduction reactions, which were of greater importance on sampling day 356 (in the summer, Fig. SI–3 of the SI document). This also led to an increase in sulfide ion concentrations (Chapelle et al., 1995). During extreme autumn rainfalls (days 400 to 449, Fig. 3A) high LA injection was maintained (between 0.65 and 0.80 mol/day, Fig. 3A). These rainfalls initially resulted in an increase in

sulfate concentration in groundwater, but a progressive decrease in this ion was observed due to the sulfate-reducing conditions in the medium, generated by the injected LA and the presence of well-developed sulfate-reducing microorganisms. Accompanying the sulfate decline, sulfide ions increased in the groundwater (Fig. SI–3C, D of the SI document).

3.3.7. Genera of microorganisms associated with sulfate reduction

The genera *Sulfurospirillum*, *Bdellovibrio*, *Treponema*, and *Desulfovibrio* (Castro et al., 2000; Fig. 6) were among the sulfate-reducing genera detected. In P2, the maximum percentage of sulfate-reducing identified genera (Fig. 6A), especially *Sulfurospirillum* (Guerrero-Barajas and Garcia-Peña, 2010; Goris and Diekert, 2016; Xu et al., 2017), coincided with highly reducing conditions in the summer season (Fig. 5). The presence of *Bdellovibrio* (Rahm et al., 2006; Moons et al., 2009; Biderre-Petit et al., 2011) tended to remain constant in P2. The remaining genera identified in P2, *Treponema* and *Desulfovibrio*, can use H_2 as a substrate, although preferring lactate (Heidelberg et al., 2004), which is consistent with the fact that lactate in the form of LA was injected into well P2. In the microcosm experiment conducted by Herrero et al. (2019), see Sections 1 and 3.1, biostimulation with LA was used. In this experiment, it was shown that the genus *Desulfovibrio* could grow under elevated PCE along with reductive dechlorinating microorganisms. This involves a syntrophic relationship where sulfate-reducing bacteria (in this case *Desulfovibrio*) can produce H_2 (under low or no sulfate presence), which is used by the dechlorinating microorganisms to reduce chloroethenes (Drzyzga and Gottschal, 2002).

In extraction well P1 in the TZBA, the genus *Thermofilum* (Mehta and Satyanarayana, 2013) was observed, presenting a significant development during the summer season, especially in the sampling of day 321 (Fig. 6C), which coincided with an increase in sulfide ion concentrations due to sulfate-reduction reactions.

At the interface with the BA (port F17-UB, Fig. 6B), towards the end of the summer period, the presence of *Treponema* increased (Menon and Voordouw, 2018; Zeng et al., 2019) which indicates that in this zone sulfate-reduction conditions lasted longer than in the upper part of the TZBA, contributing to a greater decrease in sulfate concentrations. Another genus, *Peredibacter* (Cheng et al., 2017; Kim et al., 2020), increased its presence with the increase in moles of LA injected between two successive sampling surveys, although its degree of development was not very significant.

3.3.8. Isotopic compositions of methane

The isotopic composition of methane (CH_4), Fig. SI–4 of the SI document, reveals that, at P2 and TZBA, isotopic fractionation of this gas occurred in groundwater at the recirculation cell. This fractionation was different from that of the organic compounds at the site, as most methane originated from the successive fermentation of lactate to acetate (Downey et al., 2011; He and Su, 2015; Schaefer et al., 2018). Moreover, the highest methane isotopic fractionation occurred in the summer season at P2 and at the interface between the TZBA and the BA (Fig. SI–4 of the SI document), which confirms that the injection of LA promoted the fermentation processes and the reducing conditions in the environment.

3.3.9. Genera of microorganisms associated with fermentation processes

Fig. 6A, C shows the main fermenting microorganisms detected at P2 and P1, and port F1-7UB at the interface with the BA. Among these, the genus *Truepera* (Hao et al., 2016; Xin et al., 2019) showed the greatest percentage of identification. It was detected at 0 days, although it increased significantly in summer (at P2, F1-7UB, and P1, Fig. 6A, B, C), and it ensured that lactate was fermented, favoring the bioavailability of electrons to carry out reduction reactions (Petrangeli et al., 2016). To a lesser extent, an increase in the presence of *Prevotella* was also detected in summer because of the increased LA injection rate (Fig. 3A).

3.4. Chloroethene concentrations and isotopic compositions

According to the analysis of the previous state of the medium at the interface between the TZBA and the BA, where discontinuous pools of DNAPL-PCE in free-phase and residual-phase occur (pools in a mature stage of evolution, see end of Section 1), 99.82 % of the original DNAPL is composed of PCE (Puigserver et al., 2016).

3.4.1. Evolution of PCE molar concentrations and their isotopic composition

The maximum PCE concentrations were recorded at port F1-7UB (Fig. 7A), i.e., in the interface zone between the TZBA and the BA), hence coinciding with the mature residual-phase PCE pools previously detected. Fig. 7A also shows how the PCE molar concentrations in the zone of influence of the recirculation cell decreased dramatically throughout the pilot test.

This significant decrease of PCE in F1-7UB (Fig. 7A) was detected from day 222 (73 days since cell operation) and coincided with an increase in denitrification rates (see Section 3.3.1 in the main text and Fig. SI–1A of the SI document), consistent with the fact that reductive dehalogenation of PCE to TCE initiates under denitrifying redox conditions (Bradley and Chapelle, 2010). Minimum PCE concentrations were recorded during the summer (Fig. 3A), coinciding with Fe- and sulfate-reducing redox conditions (see Sections 3.3.3, 3.3.6, and Fig. 5). An increase in PCE occurred, especially at P1 and FI-7UB (Fig. 7A), during the extreme rainfall episodes of autumn (period corresponding to 427, 449, and 464 days, Fig. 3A). These episodes caused a rise in the water table immediately upgradient of the pilot test location where the contaminated aquifer formation was unconfined. This resulted in the dissolution of PCE in pools located in the unsaturated zone. However, before these episodes of extreme precipitation, highly reducing conditions were already reached in the zone of influence of the recirculation cell, which led to rapid degradation of the mobilized PCE, and hence a dissolution process was maintained over the whole period of cell operation, as shown in Fig. 7A for the latest sampling survey conducted at the end of the test, in January (sampling day 504). This proves that it is possible to mobilize the recalcitrant sources of DNAPL accumulated in the transition zones (first working hypothesis). Although this significant decline in PCE concentration was observed in all ports of the TZBA, it was the greatest in the F1-7UB port. This is due to the evolution of the PCE pool located at the interface with the BA. As mentioned before, this was a mature pool (according to Puigserver et al., 2016) around which a bacterial biofilm was situated (Stroo et al., 2014), responsible for the existence of a PCE concentration gradient between the DNAPL pool and the groundwater, similar to what was described by ITRC (2008). The PCE was isotopically lighter in the F1-7UB port ($\delta^{13}C$ of -28.7 ± 0.5 ‰) than in the other F1UB ports because this port was located inside the DNAPL pool (Song et al., 2002; Puigserver et al., 2014). In fact, during the operation of the recirculation cell (and again in line with the demonstration of the first working hypothesis) a significant part of the pool was flushed and degraded, which allowed the mobilization, as a result of the enhanced dissolution, of a significant part of the PCE DNAPL, partially or completely saturating the porosity.

In the reinjection well (P2), a slightly different evolution of PCE concentrations than in F1-7UB was observed, as dissolved PCE from the upgradient of P2 could reach the deepest part of this well. However, the high reducing conditions of the medium (Figs. 3B, C, and 5) favored rapid biodegradation of this PCE, which was accompanied by higher isotopic fractionation (Fig. 7B), in line with that reported by Slater et al. (2001), Jørgensen (2007), Herrero et al. (2019), and Schaefer et al. (2018).

3.4.2. Degradation products of the original PCE

The evolution of TCE molar concentrations (Fig. 8A) shows how the injection of mZVI favored the increase in concentrations of lighter TCE (e.g., in FI-5UB on day 99, with a $\delta^{13}C$ value of TCE of -28.8 ± 0.5 ‰, not shown in Fig. 8) than the PCE from which it originated (-28.7 ± 0.5 ‰, the lightest value among those recorded in F1UB ports), as reported by Smith and Wang (2010), Puigserver et al. (2011), Schmidt and Jochmann (2012), and Badin et al. (2018). The TCE rapidly degraded, which favored the final isotopic composition of TCE to be heavier ($\delta^{13}C$ of -23.1 ± 0.2 ‰, not shown in Fig. 8) than that of the original PCE (the previously mentioned $\delta^{13}C$ value of -28.7 ± 0.5 ‰).

The degradation pathway of PCE in the presence of mZVI frequently results in dichloroacetylene (Van Hullebusch et al., 2020), although there

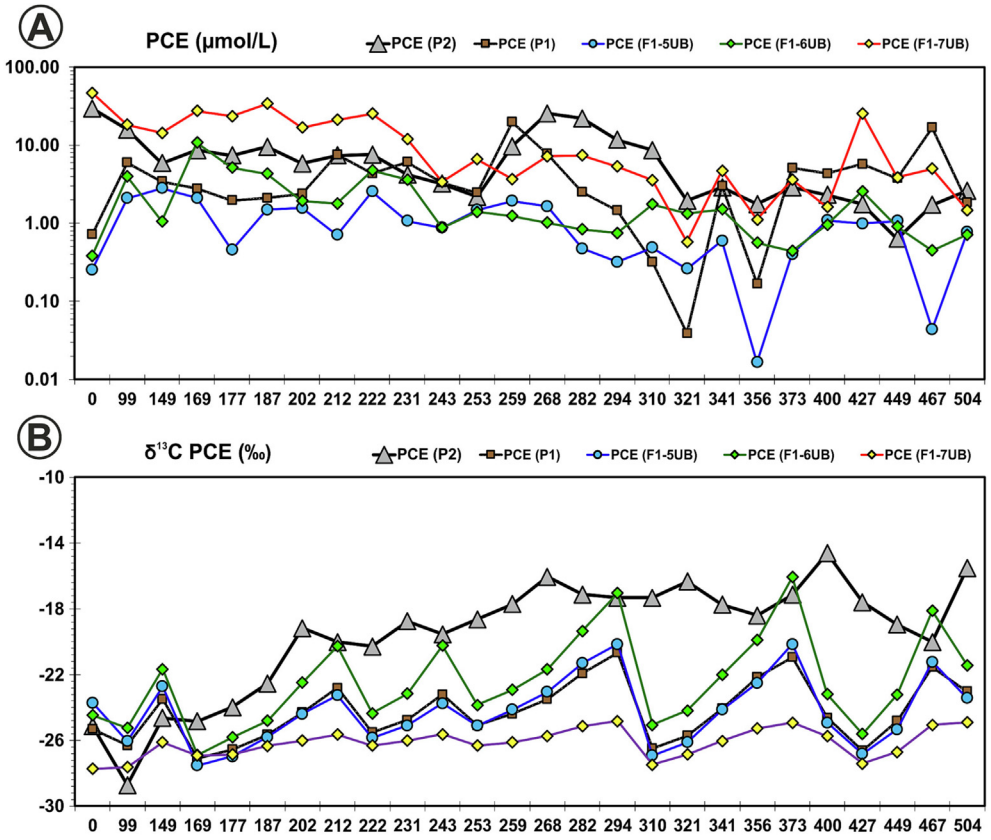

Fig. 7. Evolution throughout the pilot test of (A) molar concentrations of PCE, and (B) $\delta^{13}C$ (‰) values of PCE.

is also a minor pathway that can generate TCE. Rapid degradation of the TCE formed can generate, mostly biotically, cDCE (Pant and Pant, 2010; Hwang et al., 2015), or abiotically, chloroacetylenes (He et al., 2015; Berns et al., 2019). In both cases, the degradation produces isotopic fractionation, which can lead to an overall fractionation of TCE greater than that of the PCE from which it derives (Lojkasek-Lima et al., 2012; Gafni et al., 2018). This is especially noteworthy in the case of the pool that was treated during the pilot test, where a masking effect of the light PCE, incorporated by the enhanced dissolution of that pool (Song et al., 2002; Puigserver et al., 2014), occurred upon mixing with the heavy PCE that accumulated in the reservoir as a result of the degradation of this compound to isotopically lighter products (Van Breukelen et al., 2005; Amaral et al., 2011; Wiegert et al., 2013). This caused the PCE recorded in the pool to show lower isotopic fractionation than would be expected, making it difficult to determine its degradation rate.

Abiotic degradation products belonging to the chloroacetylenes group are very unstable compounds (Butler and Hayes, 2001; He et al., 2015; Dong et al., 2019). Despite this, before the operation of the recirculation cell, the isotopic composition of dichloroacetylene was already determined in F1-7UB ($\delta^{13}C$ of -26.5 ± 0.8 ‰), with lighter values than that of the original PCE ($\delta^{13}C$ of -28.7 ± 0.5 ‰). After cell activation, the presence of chloroacetylenes was detected, although their isotopic fractionation could not be determined, except for chloroacetylene after 356 days at port F1-7UB ($\delta^{13}C$ of -3.1 ± 0.8 ‰), indicating that much of the chloroacetylenes formed were rapidly degraded.

The progressive increase in TCE concentrations, especially during the summer period because of a higher rate of biotic degradation of PCE (Fig. 7B), occurred from the beginning of the pilot test, as reductive dechlorination of PCE to TCE is initiated under denitrification conditions (Weatherill et al., 2019) that already were occurring naturally at the site. Fig. 7A also shows how the PCE degrading effect of mZVI injection was persistent over time, as high TCE concentrations were recorded up to day 222 (in the spring), and became significant again during the summer, extending until November 2018 (on day 427, Fig. 8A). The highest TCE degradation in the TZBA was recorded at port F1-7UB. In this port, the initially generated TCE had a lighter character ($\delta^{13}C$ of -31.5 ± 0.2 ‰, on day 99) than that of the original PCE (-28.7 ± 0.5 ‰). However, rapidly that TCE became heavier, recording an isotopic composition with a $\delta^{13}C$ value of -16.9 ± 0.7 ‰ on day 212. Considering the errors in determining these two values of $\delta^{13}C_{TCE}$, (on days 99 and 212) the calculation of $\Delta\delta^{13}C_{TCE}$ resulted in a range of values from 14.1 ‰ to 14.6 ‰. This range was much higher than in the case of $\Delta\delta^{13}C_{PCE}$ for the same port between days 0 and 212 (a range from 2.7 ‰ to 3.5 ‰). From day 222 to 373, a progressive increase in TCE was recorded in ports of multilevel well F1UB, accompanied by increases in cDCE (Fig. 8B), since under Mn-reducing conditions, and especially Fe-reducing conditions, Fig. SI–2B, D of the SI document (such as those that occurred in summer, see Section 3.3.3 and Fig. 5), TCE degrades quickly to cDCE by biotic reductive dechlorination (Wei and Finneran, 2011; Němeček et al., 2020). This, which would normally result in the accumulation of cDCE in the medium, did not occur, as no high concentrations of either cDCE or TCE were observed in ports of the multilevel well F1UB (see the last three samplings, on days 449, 464, and 504 in Fig. 8). In contrast, elevated concentrations were observed in the reinjection well (P2), where only biotic degradation took place. The low concentrations of TCE and cDCE in the F1UB ports suggest a high degradation rate of chloroethenes (of PCE, via dichloroacetylene; and of TCE, via chloroacetylene and subsequently to acetylene), as reported by Van Hullebusch et al. (2020). However, metabolic degradation of these compounds by the microbial content in the area should not be ruled out (see Section 3.5.2).

Fig. 8A also shows that after the extreme rainfall recorded during October and November 2018 (Fig. 3A, autumn), on day 449, TCE concentrations in P1 and ports 5 and 6 of F1UB decreased. Three factors accounted for this decrease: i) the dilution effect; ii) the consequent oxygenation of the medium, which hinders reductive dechlorination, especially that of PCE to TCE; and iii) the oxidative dechlorination resulting from the activity of

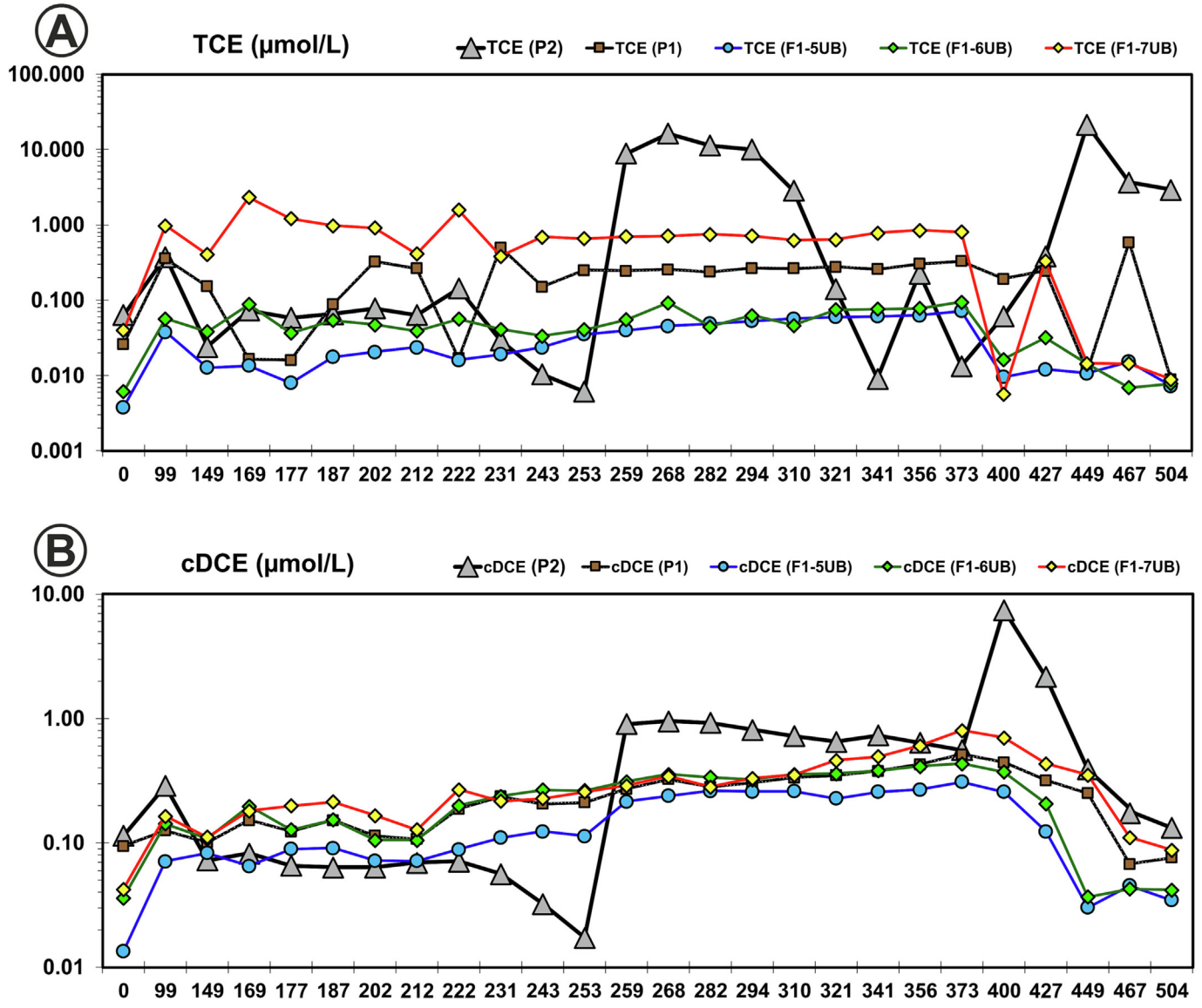

Fig. 8. Evolution throughout the pilot test of (A) molar concentrations of TCE, and (B) molar concentrations of cDCE.

microorganisms that oxidize the less oxidized chloroethenes (TCE, cDCE, and VC; see Section 3.5.2).

In F1-7UB, the deepest port of F1UB, Fig. 8 shows that the reducing conditions and the well-developed dechlorinating microbial flora generated during the summer allowed the PCE that was subsequently incorporated into the groundwater flow by pool flushing (when the rise in the water table occurred because of rainfalls) to degrade rapidly to TCE and to cDCE (Fig. 8A, B). Evidence of this significant PCE degradation in the TZBA was also found in the extraction well (P1), where increases in TCE concentration were also recorded following the substantial piezometric level rise.

Fig. 8A further shows how the maximum TCE concentrations in the reinjection well (P2) were recorded in May and June (between days 259 and 294, i.e., between late spring and early summer), when the dominant redox conditions in this well were methanogenic (Fig. SI–4B of the SI document), hence compatible with Mn to Fe reduction processes (Fig. SI–2B, C of the SI document) and with the degradation of PCE to TCE (Figs. 7A and 8A). From day 294 to 373 (June to September, summer season), when dominant redox conditions changed from sulfate-reducing (Fig. SI–3B) to methanogenic (Fig. SI–4B of the SI document) in the reinjection well (P2), TCE concentrations decreased because of the degradation of this compound (Wei and Finneran, 2011; Butler et al., 2013). This process coincided with significant concentrations in cDCE (Fig. 8B) and a rise in TCE isotopic fractionation (data not shown in figures). During the extreme rainfall events of October and November 2018, between days 400 and 449 (autumn) and after (Fig. 3A), TCE concentrations in P2 recovered again, as redox conditions reverted to Mn-reducing, while the microbial flora remained well developed.

Fig. 8B shows that in the extraction well (P1) in the TZBA, the increase in cDCE was progressive and especially prominent during the summer period (from day 294 to 373), when conditions evolved from Fe-reducing to sulfate-reducing. This increase in cDCE was not accompanied by a parallel increase in VC, but rather by an increase in acetate, suggesting that when cDCE degrades, it does not give rise to VC, but rather that the presence of mZVI in the environment favors the abiotic degradation of cDCE, and VC to less toxic products as chloroacetylenes (He et al., 2015; Berns et al., 2019). This makes the combined use of the two remediation techniques used at the same time particularly interesting, demonstrating that the coupled strategy at the field scale can be applied efficiently, thus confirming the validity of the second working hypothesis. This is the main novelty of the current work. Certainly, the literature does not report examples of combined techniques, such as those analyzed herein, in transition zones to bottom aquitards in which PCE DNAPL pools accumulated. This novelty may represent a significant positive impact for society and the environment,

since this combined strategy may be efficiently implemented in transition zones where the accumulated pools are currently extremely recalcitrant and are still causing groundwater pollution in aquifers laterally connected to and located downgradient of such zones.

As in the case of TCE, extreme rainfalls in October and November 2018 (Fig. 3A) caused cDCE concentrations to decrease drastically, although a slight increase in this compound was subsequently observed because of increased degradation of PCE and TCE.

In the reinjection well (P2), the most reductive conditions (Fig. 3B, C) favored elevated cDCE concentrations (Fig. 8). Since this well is upgradient of the mZVI injection boreholes, PCE here was mostly degraded by biotic reductive dechlorination (Kranzioch et al., 2013; Patil et al., 2014; Nijenhuis and Kuntze, 2016). The existence of a well-developed microbial flora capable of degrading PCE explains why cDCE concentrations also increased significantly after the flushing of pools of PCE due to the raised water table caused by major rainfall events.

Regarding VC, it should be noted that in general its presence was detected in the multilevel wells, but in concentrations below the quantification limit, 0.0021 μmol/L. In contrast, elevated VC concentrations were detected in the reinjection well (P2), where during the last three sampling surveys, on days 449, 467, and 504 (end of the pilot test), molar concentrations of VC (not shown in figures) declined markedly, from the maximum concentration of 6.81 μmol/L on day 449 to 0.12 μmol/L on day 504.The concentrations of cDCE at P2 also decreased between these two days, from 0.39 μmol/L to 0.012 μmol/L (Fig. 8B). It should be emphasized that the reinjection well (P2) was not used to monitor the combined strategy, since it was located upgradient of the mZVI injection points (therefore only biotic degradation occurred). The most harmful compounds (cDCE and VC) were eliminated downgradient as they moved through the zone where mZVI was injected.

The low concentrations of cDCE and VC in ports of the multilevel wells and the formation of chloroacetylenes (dichloroacetylene and chloroacetylene, which convert to acetylene) prove that the presence of mZVI in the zone of influence of the recirculation cell favors the degradation of chloroethenes, minimizing the production and accumulation of VC as the most harmful degradation product, which once again validates the second working hypothesis.

3.5. Microorganisms associated with the degradation of chloroethenes

3.5.1. Genera responsible for reductive processes

Herrero (2015) and Puigserver et al. (2016), in sediment samples from boreholes B-F1UB and B-F2UB where the multilevel wells F1UB and F2UB were installed (which were used to monitor the current pilot test), identified two genera of microorganisms potentially involved in the reductive dechlorination of chloroethenes. These were *Dehalococcoides* (Rossi et al., 2012; Nijenhuis and Kuntze, 2016; Saiyari et al., 2018), and *Geobacter* (Löffler et al., 2013; Cápiro et al., 2015; Němeček et al., 2017). These two dehalogenating reductive genera were also identified in groundwater samplings of the pilot test (Fig. 9A). In the reinjection well (P2), *Geobacter* was identified during the summer season (Fig. 9A) only on days 294 and 321 (Fig. 3A), although with relatively low identification percentages. *Sulfurospirillum* (Buttet et al., 2013; Goris and Diekert, 2016) was detected in this well after the start of the LA injection, with the highest identification percentage (in the sampling on day 169), and in general, its identification percentage remained high throughout the different samplings. The genus *Treponema* (Lee and Lee, 2016) was also identified in P2, where other microorganisms belonging to the phylum Chloroflexi were detected, but whose genera could not be identified.

The genus *Dehalococcoides*, a member of the phylum Chloroflexi, is a strict halorespirator of organochloride compounds (Nijenhuis and Kuntze, 2016). This genus was detected in port FI-7UB of the multilevel well F1UB, in the interface TZBA-BA, with a maximum percentage of identification of sequences of 1.5 % of the total number of microorganisms detected (obtained during the summer, Fig. 9A). Furthermore, as in the case of P2, other microorganisms belonging to the Chloroflexi phylum were detected in this port, although their genera could not be identified. These microorganisms constituted between 4 % and 8 % of the community in all the groundwater samples collected in the mentioned port.

Thus, the maximum percentages of identification of dehalogenating genera by halorespiration occurred (or were only detected) in the zone of the TZBA-BA interface. This zone includes the FI-7UB port, but also the deepest part of the extraction well P1 (although in this case the genera could not be identified, they were only detected, Fig. 9A). These maximum identification percentages occurred during the summer, with *Dehalococcoides* and *Treponema* in FI-7UB. However, reductive dechlorination also occurred in P2 during the summer, with *Geobacter*, *Sulfurospirillum*, and *Treponema*. All of these highlight that biotic reductive dechlorination occurs in the reinjection well P2 and at the TZBA-BA interface (in the latter case in agreement with what was observed by Puigserver et al. (2016).

3.5.2. Genera responsible for oxidative processes

Throughout the pilot test, genera potentially performing oxidative dechlorination were detected in the TZBA (P1) and port F1-7UB in the interface with the BA (Fig. 9A). By contrast, in P2, where anoxic conditions were maintained throughout the pilot test because of the injection of LA, the presence of oxidizing genera was small and attributable to the reinjection of groundwater from P1. It is very likely that in P2, these oxidizing microorganisms were not active due to the mentioned anoxic conditions, which explains why the VC produced by biostimulation accumulates or degrades via biotic reductive dechlorination (Kim et al., 2010; Löffler et al., 2013).

In the interface with the BA (F1-7UB), recorded in summer, and with high identification percentages (Fig. 9A), were the genera *Nocardiodes* (Schmidt et al., 2014; Thornton et al., 2016), *Aciditerrimonas* (Pant and Pant, 2010; Fullerton et al., 2014; Gafni et al., 2020), *Phenylobacterium*, and *Nitrosospira*. Lower identification percentages were also recorded in port F1-7UB in summer for *Brevundimonas* (Wilson et al., 2016), *Burkholderia* (Peng and Shih, 2013; Gaza et al., 2019; Gafni et al., 2020), *Sediminibacterium* (Wilson et al., 2016), and *Variovorax* (Wilson et al., 2016).

Regarding the extraction well (P1), the following genera were recorded in summer, also with high identification percentages (Fig. 9A): *Aciditerrimonas*, *Nitrosospira*, and *Nocardioides* (Gafni et al., 2020). With lower identification percentages, also recorded were *Brevundimonas* (Wilson et al., 2016), *Burkholderia* (Peng and Shih, 2013; Gaza et al., 2019; Gafni et al., 2020), and *Phenylobacterium* (Wilson et al., 2016).

Thus, except for the area closest to P2, within the zone of influence of the recirculation cell, the existence of positive ORP values and DO in summer (Fig. 3 B, C), and especially after the high rainfall events during autumn and early winter (Fig. 3A), made possible the presence of aerobic oxidizing microorganisms capable of biodegrading the transformation products of the biotic reductive dechlorination of PCE, TCE, and cDCE (and VC) to CO_2 (Tiehm and Schmidt, 2011), even in the zone of the TZBA-BA interface. This would indicate that a significant part of the TCE and cDCE produced by incomplete biological degradation of PCE was transformed to CO_2. This would be comparable to a certain coupling between biotic reductive and oxidative degradation processes (i.e., between microorganisms that reduce and oxidize chloroethenes, respectively), which would play a similar role to that stated by the second working hypothesis and suggesting the validity of the third working hypothesis.

3.6. Percentage degradation of the original PCE

The fficiency in the degradation of the original PCE in the zone of influence of the recirculation cell after mZVI injection was finished (day 0, Fig. 3A) throughout the pilot test, is found in Table 1. This efficiency is shown as a percentage of PCE degradation (B%, see Section 3.2 in the SI document) for the reinjection well P2, ports F1-5UB, F1-6UB, and F1-7UB of the multilevel well F1UB and extraction well P1. The table also shows for the same monitoring points the enrichment factor (ϵ‰) values. The degradation B% values ranged from 16 % to 43 % in ports F1-5UB, F1-6UB, and F1-7UB of the multilevel well F1UB, and extraction well P1 on day 99 (when the combined strategy had not yet been implemented, as only mZVI was operating and the recirculation cell had not started up yet).

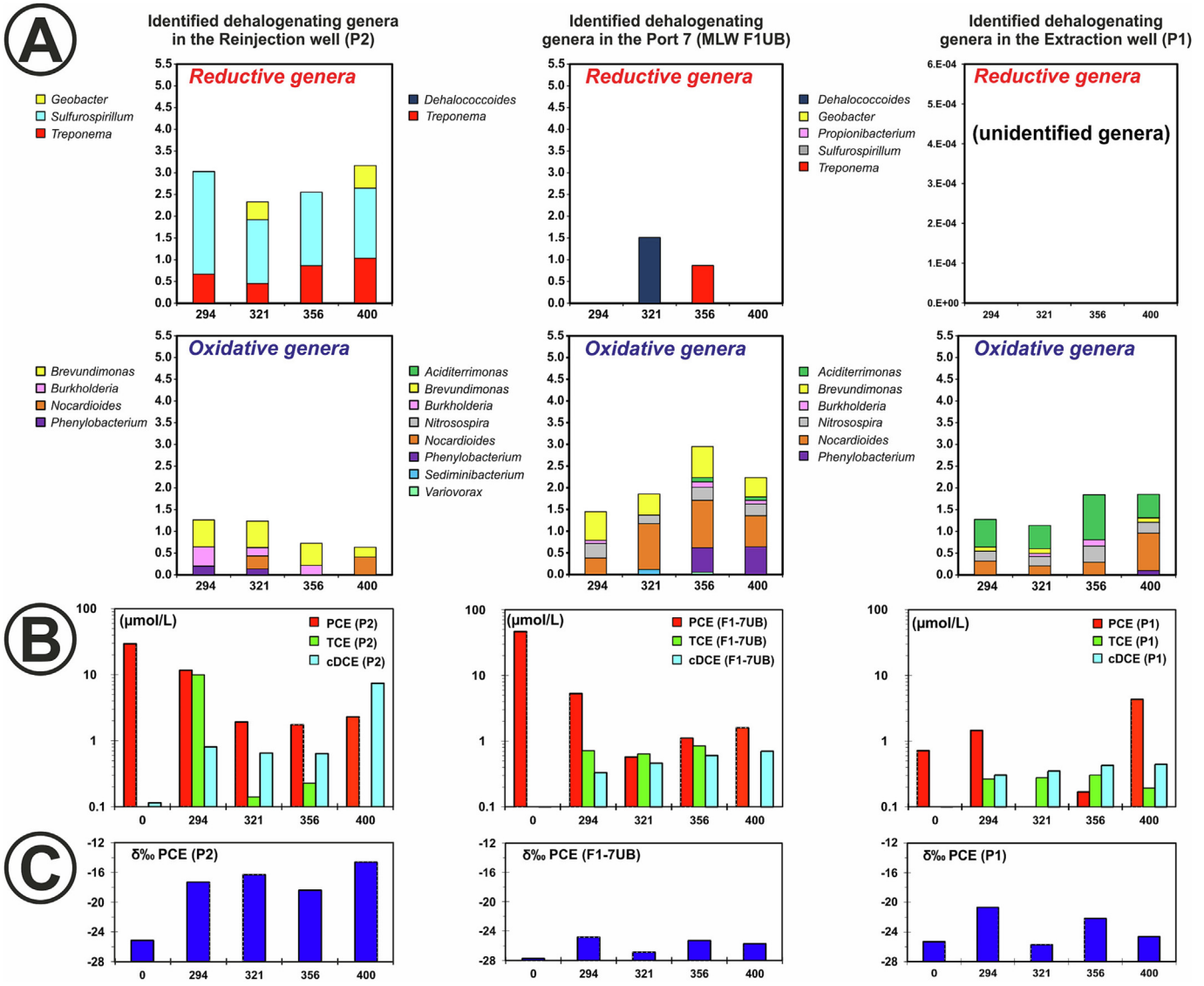

Fig. 9. (A) Bacterial genera identified during summer sampling days; X-axis: sampling day; Y-axis: percentage that each genus represented within the identified bacterial community; (B) evolution of molar concentrations of PCE, TCE, and cDCE on the day before the start of the pilot test (day 0) and during the same summer sampling days; (C) $\delta^{13}C$ (‰) values of PCE on the day before the start of the pilot test (day 0) and during the same summer sampling days.

The B value of 9.7 % (Table 1) in reinjection well P2 has not been considered for two reasons: i) only biostimulation of the bacterial flora occurred there, as mentioned previously, and ii) the concentrations of the incomplete transformation products of PCE in P2 at the end of the test (day 504) were higher than those at day 99 (day 504, Fig. 8). In addition, it should be noted that the ϵ‰ and B% data are partially masked values since, during the test, PCE was continuously mobilized by enhanced dissolution from the pool, whose PCE is isotopically light, which underestimates the real value of the percentage of degradation B%. Keeping in mind the masking of degradation percentage data (B%), Table 1 also shows that at the end of 400 days between 83.4 % and 96.3 % of PCE of the original PCE in the TZBA had already been degraded, which proves that it is possible to mobilize the recalcitrant sources of DNAPL accumulated in the transition zones (once more proving the first working hypothesis). In Table 1, the period after day 400 (i.e., from day 401 to day 504, end of the test) was not included due to the input of considerable PCE from pool flushing when the water table rose due to the significant rainfall that occurred (Fig. 3A).

Moreover, it must be considered that these values only correspond to the mobilization of the PCE that was in the form of a free or residual-phase. They do not account for the percentage of PCE stored in the porewater of fine sediments in the TZBA (or, in the UPA, in the coarse sediments with a fine matrix), nor sorbed in the particulate organic matter of all these materials.

4. Conclusions

1) Following the activation of the recirculation cell, a rapid enhanced degradation-dissolution PCE DNAPL process initiated that led to the mobilization of the DNAPL pool. This process was maintained throughout the cell operation period.
2) The LA biostimulation of the halorespiring activity of genera of chlorinated solvents reducing microorganisms of the medium (*Dehalococcoides*, *Geobacter*, *Sulfurospirillum*, and *Treponema*) promoted the incomplete biotic reductive dechlorination of PCE, leading to the formation of TCE, cDCE, and VC, which are more harmful products than the parent PCE.
3) The occurrence of genera of chlorinated solvents oxidizing microorganisms under the oxic conditions generated by the oxygen supply during the recharge periods of part of the rainfall (*Nocardiodes*, *Aciditerrimonas*, *Phenylobacterium*, and *Nitrosospira*) enabled the oxidation of TCE, cDCE, and VC, avoiding the accumulation of these harmful transformation products. This would be comparable to a certain coupling between biotic reductive and oxidative degradation processes.

Table 1
Percentage of original PCE (that which existed on day 0) degraded throughout the pilot test; enrichment factor (ϵ) values denote the continuous input of new PCE incorporated into the groundwater from the PCE pool.

Time since start of pilot test (days)	P2	F1-5 UB	F1-6UB	F1-7UB	P1
	Enrichment factors (‰)				
	−4	−4	−4.5	−2	−4
	PCE degraded during the pilot test (B%)				
0	0.0	0.0	0.0	0.0	0.0
99	9.7	43.1	16.00	41.3	25.5
149	5.0	41.6	47.28	60.2	43.7
169	30.1	54.8	43.08	45.9	32.6
177	51.7	69.9	58.12	67.6	51.7
202	74.8	76.7	72.38	92.9	55.9
212	72.3	70.7	83.22	89.9	59.6
222	70.4	69.4	79.16	87.9	72.4
231	79.9	70.0	77.76	89.4	71.0
240	78.9	65.9	78.71	83.7	71.7
253	77.0	64.1	75.31	81.9	68.7
259	81.3	74.1	73.55	90.2	66.2
294	86.1	76.1	82.85	91.9	71.4
321	89.2	79.2	86.19	94.3	73.8
341	88.4	78.1	84.74	93.1	77.5
356	87.6	77.2	84.27	91.9	74.5
373	91.5	81.3	87.10	94.1	77.2
400	93.0	84.1	89.79	96.3	83.4

4) The mZVI injected into the TZBA abiotically degraded PCE and the other products from their biotic degradation (TCE, cDCE, and VC) transforming them into chloroacetylenes. The latter were converted into the harmless acetylene.
5) After 400 days from the start of the recirculation cell, removal efficiencies ranging from 83.4 % to 96.3 % of the PCE from the PCE pool in the zone of influence of the cell were obtained. The degradation of this PCE was virtually complete, leading to harmless compounds that derived to CO_2.
6) The pilot test has shown that a coupling and interdependence between biotic and abiotic processes has occurred. This has allowed the generation of the necessary synergies for the efficient mobilization of recalcitrant pools in transition zones from the aquifer to the bottom aquitard, which is the main novelty of the current research.
7) Therefore, the combined use of mZVI and LA biostimulation of the indigenous microorganisms is a very efficient strategy for the removal of these pools. This, potentially represents a significant positive impact for society and the environment, as the combined strategy could be efficiently applied in other transition zones affected by the accumulation of DNAPL pools of other compounds different from PCE.
8) In the combined strategy, the LA (or other more suitable carbon and energy source for each case) addition regime in the natural environment has to be adapted according to changing environmental conditions to promote the most efficient biotic degradation of pollutants.

CRediT authorship contribution statement

Diana Puigserver: She executed and testified the boreholes to inject mZVI and construct extraction end reinjection wells. She periodically collected the groundwater needed for the monitoring of the pilot test. She also performed the chemical and isotopic analyzes of these groundwater samples and processed the data, participated in the discussion meetings on the results obtained with the other two authors, and wrote the manuscript.

Jofre Herrero: He participated in the periodic collection of the groundwater saples needed for the monitoring of the pilot test. He performed the detection and identification analyses of microorganisms and the different molecular techniques necessary for this purpose in groundwater periodically sampled during the pilot test. He participated in the discussion meetings of the results obtained together with the other two authors.

José M. Carmona: He designed the boreholes to inject mZVI. He also designed the recirculation cell and participated in the execution of the research drilling boreholes, in the testification, and in their equipment as piezometers. He designed and made the calculations to inject the reactants in the transition zone. He also supervised the progress of the research and participated in the meetings to discuss the results obtained with the other two authors. He super vised the redaction of the manuscript and was the corresponding author.

Data availability

The data that has been used is confidential.

Declaration of competing interest

The authors of this research paper (Diana Puigserver, Jofre Herrero and José M. Carmona) declare that they have no known competing financial interests or personal relationships that could have appeared to influence the work reported in this paper.

Acknowledgments

We are indebted to the Catalan Water Agency (ACA) and to the members of INTERFREN of Figueres and INTECSON S.L. of Reus for their support and cooperation while carrying out the field work. We should also like to thank the colleagues of the Department of Mineralogy, Petrology and Applied Geology of the University of Barcelona and, especially, the members of the Environmental Hydrogeology and Global Change group of that department. We are grateful to the personnel of the Scientific Technical Services of the University of Barcelona for their help in analyzing the samples. We should also like to acknowledge the institution funding the research carried out within the following project: CTN1601136 (Catalan Water Agency, ACA).

Appendix A. Supplementary data

Supplementary data to this article can be found online at https://doi.org/10.1016/j.scitotenv.2023.162751.

References

ACA, 2019. Pla de gestió 2022-2027. Memòria. Estudi general de la demarcació, anàlisi d'impactes i pressions de l'activitat humana, i anàlisi econòmica de l'ús de l'aigua a les masses d'aigua al Districte de conca fluvial de Catalunya. Document Impress 2019.
Ahmed, M., Lin, O., Saup, C.M., Wilkins, M.J., Lin, L.S., 2019. Effects of Fe/S ratio on the kinetics and microbial ecology of an fe (III)-dosed anaerobic wastewater treatment system. J. Hazard. Mater. 369, 593–600.
Amaral, H.I., Aeppli, C., Kipfer, R., Berg, M., 2011. Assessing the transformation of chlorinated ethenes in aquifers with limited potential for natural attenuation: added values of compound-specific carbon isotope analysis and groundwater dating. Chemosphere 85 (5), 774–781.
Antoniou, K., Mamais, D., Pantazidou, M., 2019. Reductive dechlorination of trichloroethene under different sulfate-reducing and electron donor conditions. J. Contam. Hydrol. 226, 103519.
Appelo, C.A.J., Postma, D., 1996. Geochemistry, Groundwater and Pollution (3rd Corrected Print). Balkema, Rotterdam, p. 536.
Atashgahi, S., Lu, Y., Ramiro-Garcia, J., Peng, P., Maphosa, F., Sipkema, D., Springael, D., 2017. Geochemical parameters and reductive dechlorination determine aerobic cometabolic vs aerobic metabolic vinyl chloride biodegradation at oxic/anoxic interface of hyporheic zones. Environ. Sci. Technol. 51 (3), 1626–1634.
Aulenta, F., Canosa, A., Leccese, M., Petrangeli Papini, M., Majone, M., Viotti, P., 2007a. Field study of in situ anaerobic bioremediation of a chlorinated solvent source zone. Ind. Eng. Chem. Res. 46 (21), 6812–6819.
Aulenta, F., Pera, A., Rossetti, S., Papini, M.P., Majone, M., 2007b. Relevance of side reactions in anaerobic reductive dechlorination microcosms amended with different electron donors. Water Res. 41 (1), 27–38.
Badin, A., Braun, F., Halloran, L.J., Maillard, J., Hunkeler, D., 2018. Modelling of C/Cl isotopic behaviour during chloroethene biotic reductive dechlorination: capabilities and limitations of simplified and comprehensive models. PLoS One 13 (8).
Baek, G., Kim, J., Shin, S.G., Lee, C., 2016. Bioaugmentation of anaerobic sludge digestion with iron-reducing bacteria: process and microbial responses to variations in hydraulic retention time. Appl. Microbiol. Biotechnol. 100 (2), 927–937.
Baskaran, D., Rajamanickam, R., 2019. Aerobic biodegradation of trichloroethylene by consortium microorganism from Turkey litter compost. J. Environ. Chem. Eng. 7 (4), 103260.

Benioug, M., Golfier, F., Fischer, P., Oltean, C., Buès, M.A., Yang, X., 2019. Interaction between biofilm growth and NAPL remediation: a pore-scale study. Adv. Water Resour. 125, 82–97.
Berns, E.C., Sanford, R.A., Valocchi, A.J., Strathmann, T.J., Schaefer, C.E., Werth, C.J., 2019. Contributions of biotic and abiotic pathways to anaerobic trichloroethene transformation in low permeability source zones. J. Contam. Hydrol. 224, 103480.
Biderre-Petit, C., Boucher, D., Kuever, J., Alberic, P., Jézéquel, D., Chebance, B., Peyret, P., 2011. Identification of sulfur-cycle prokaryotes in a low-sulfate Lake (Lake Pavin) using aprA and 16S rRNA gene markers. Microb. Ecol. 61 (2), 313–327.
Blöthe, M., Roden, E.E., 2009. Microbial iron redox cycling in a circumneutral-pH groundwater seep. Appl. Environ. Microbiol. 75 (2), 468–473.
Bradley, P.M., 2003. History and ecology of chloroethene biodegradation: a review. Bioremediat. J. 7 (2), 81–109.
Bradley, P.M., 2012. Microbial Mineralization of cis-Dichloroethene and Vinyl Chloride as a Component of Natural Attenuation of Chloroethene Contaminants under Conditions Identified in the Field as Anoxic (No. SIR-2012-5032). Geological Survey, Reston VA.
Bradley, P.M., Chapelle, F.H., 2010. Biodegradation of chlorinated ethenes. In Situ Remediation of Chlorinated Solvent Plumes. Springer, New York, NY, pp. 39–67.
Brusseau, M.L., Matthieu III, D.E., Carroll, K.C., Mainhagu, J., Morrison, C., McMillan, A., Plaschke, M., 2013. Characterizing long-term contaminant mass discharge and the relationship between reductions in discharge and reductions in mass for DNAPL source areas. J. Contam. Hydrol. 149, 1–12.
Bruton, T.A., Pycke, B.F., Halden, R.U., 2015. Effect of nanoscale zero-valent iron treatment on biological reductive dechlorination: a review of current understanding and research needs. Crit. Rev. Environ. Sci. Technol. 45 (11), 1148–1175.
Burns, L.C., Stevens, R.J., Smith, R.V., Cooper, J.E., 1995. The occurrence and possible sources of nitrite in a grazed, fertilized, grassland soil. Soil Biol. Biochem. 27 (1), 47–59.
Butler, E.C., Hayes, K.F., 2001. Factors influencing rates and products in the transformation of trichloroethylene by iron sulfide and iron metal. Environ. Sci. Technol. 35 (19), 3884–3891.
Butler, E.C., Chen, L., Darlington, R., 2013. Transformation of trichloroethylene to predominantly non-regulated products under stimulated sulfate reducing conditions. Groundw. Monit. Remediat. 33 (3), 52–60.
Buttet, G.F., Holliger, C., Maillard, J., 2013. Functional genotyping of sulfurospirillum spp. In mixed cultures allowed the identification of a new tetrachloroethene reductive dehalogenase. Appl. Environ. Microbiol. 79 (22), 6941–6947.
Cápiro, N.L., Löffler, F.E., Pennell, K.D., 2015. Spatial and temporal dynamics of organohalide-respiring bacteria in a heterogeneous PCE–DNAPL source zone. J. Contam. Hydrol. 182, 78–90.
Castro, H.F., Williams, N.H., Ogram, A., 2000. Phylogeny of sulfate-reducing bacteria1. FEMS Microbiol. Ecol. 31, 1–9.
Cecchetti, A.R., Stiegler, A.N., Gonthier, E.A., Bandaru, S.R., Fakra, S.C., Alvarez-Cohen, L., Sedlak, D.L., 2022. Fate of dissolved nitrogen in a horizontal levee: seasonal fluctuations in nitrate removal processes. Environ. Sci. Technol. 56 (4), 2770–2782.
Çeçen, F., Kocamemi, B.A., Aktaş, Ö., 2010. Metabolic and co-metabolic degradation of industrially important chlorinated organics under aerobic conditions. Xenobiotics in the Urban Water Cycle. Springer, Dordrecht, pp. 161–178.
Chapelle, F.H., McMahon, P.B., Dubrovsky, N.M., Fujii, R.F., Oaksford, E.T., Vroblesky, D.A., 1995. Deducing the distribution of terminal electron-accepting processes in hydrologically diverse groundwater systems. Water Resour. Res. 31 (2), 359–371.
Chen, W.H., Chen, Z.B., Yuan, C.S., Hung, C.H., Ning, S.K., 2016. Investigating the differences between receptor and dispersion modeling for concentration prediction and health risk assessment of volatile organic compounds from petrochemical industrial complexes. J. Environ. Manag. 166, 440–449.
Cheng, Q., Nengzi, L., Bao, L., Huang, Y., Liu, S., Cheng, X., Zhang, J., 2017. Distribution and genetic diversity of microbial populations in the pilot-scale biofilter for simultaneous removal of ammonia, iron and manganese from real groundwater. Chemosphere 182, 450–457.
Christ, J.A., Ramsburg, C.A., Pennell, K.D., Abriola, L.M., 2010. Predicting DNAPL mass discharge from pool-dominated source zones. J. Contam. Hydrol. 114 (1–4), 18–34.
Christensen, T.H., Bjerg, P.L., Banwart, S.A., Jakobsen, R., Heron, G., Albrechtsen, H.J., 2000. Characterization of redox conditions in groundwater contaminant plumes. J. Contam. Hydrol. 45 (3–4), 165–241.
Coby, A.J., Picardal, F., Shelobolina, E., Xu, H., Roden, E.E., 2011. Repeated anaerobic microbial redox cycling of iron. Appl. Environ. Microbiol. 77 (17), 6036–6042.
Cullen, L.G., Tilston, E.L., Mitchell, G.R., Collins, C.D., Shaw, L.J., 2011. Assessing the impact of nano-and micro-scale zerovalent iron particles on soil microbial activities: particle reactivity interferes with assay conditions and interpretation of genuine microbial effects. Chemosphere 82 (11), 1675–1682.
Culpepper, J.D., Scherer, M.M., Robinson, T.C., Neumann, A., Cwiertny, D., Latta, D.E., 2018. Reduction of PCE and TCE by magnetite revisited. Environ. Sci. Process. Impacts 20 (10), 1340–1349.
Cummings, D.E., Caccavo Jr., F., Spring, S., Rosenzweig, R.F., 1999. Ferribacterium limneticum, gen. Nov., sp. Nov., an Fe(III)-reducing microorganism isolated from mining-impacted freshwater lake sediments. Arch. Microbiol. 171, 183–188. https://doi.org/10.1007/s002030050697.
Daalkhaijav, U., Nemati, M., 2014. Ammonia loading rate: an effective variable to control partial nitrification and generate the anaerobic ammonium oxidation influent. Environ. Technol. 35 (5), 523–531.
Daims, H., Wagner, M., 2018. Nitrospira. Trends Microbiol. 26 (5), 462–463.
Daims, H., Lebedeva, E.V., Pjevac, P., Han, P., Herbold, C., Albertsen, M., Kirkegaard, R.H., 2015. Complete nitrification by nitrospira bacteria. Nature 528 (7583), 504.
Dolinová, I., Štrojsová, M., Černík, M., Němeček, J., Macháčková, J., Ševců, A., 2017. Microbial degradation of chloroethenes: a review. Environ. Sci. Pollut. Res. 24 (15), 13262–13283.
Dong, Y., Liang, X., Krumholz, L.R., Philp, R.P., Butler, E.C., 2009. The relative contributions of abiotic and microbial processes to the transformation of tetrachloroethylene and trichloroethylene in anaerobic microcosms. Environ. Sci. Technol. 43 (3), 690–697.
Dong, H., Li, L., Lu, Y., Cheng, Y., Wang, Y., Ning, Q., Zeng, G., 2019. Integration of nanoscale zero-valent iron and functional anaerobic bacteria for groundwater remediation: a review. Environ. Int. 124, 265–277.
Downey, S.T., Zhai, X., Meadows, R., 2011. Field-scale Treatability Study for Enhanced In Situ Bioremediation of Explosives in Groundwater: BioBarrier Installation and Hot Spot Treatment Using DPT Injection. Shaw Group Inc, Baton Rouge LA.
Drzyzga, O., Gottschal, J.C., 2002. Tetrachloroethene dehalorespiration and growth of desulfitobacterium frappieri TCE1 in strict dependence on the activity of desulfovibrio fructosivorans. Appl. Environ. Microbiol. 68 (2), 642–649.
Dubinina, G.A., Sorokina, A.Y., 2014. Neutrophilic lithotrophic iron-oxidizing prokaryotes and their role in the biogeochemical processes of the iron cycle. Microbiology 83 (1–2), 1–14.
Ellis, P.A., Rivett, M.O., 2007. Assessing the impact of VOC-contaminated groundwater on surface water at the city scale. J. Contam. Hydrol. 91 (1–2), 107–127.
Emerson, D., Fleming, E.J., McBeth, J.M., 2010. Iron-oxidizing bacteria: an environmental and genomic perspective. Annu. Rev. Microbiol. 64, 561–583.
Fan, D., Bradley, M.J., Hinkle, A.W., Johnson, R.L., Tratnyek, P.G., 2016. Chemical reactivity probes for assessing abiotic natural attenuation by reducing iron minerals. Environ. Sci. Technol. 50 (4), 1868–1876.
Fedler, C.B., Pearson, P.R., Mueller, B., Green, C.J., 2003. Effects of denitrification on irrigated wastewater systems. 2003 ASAE Annual Meeting. American Society of Agricultural and Biological Engineers, p. 1.
Field, J.A., Sierra-Alvarez, R., 2001. Review of Scientific Literature on Microbial Dechlorination and Chlorination of Key Chlorinated Compounds. Department of Chemical & Environmental Engineering University of Arizona 37p.
Findlay, M., Smoler, D.F., Fogel, S., Mattes, T.E., 2016. Aerobic vinyl chloride metabolism in groundwater microcosms by methanotrophic and etheneotrophic bacteria. Environ. Sci. Technol. 50 (7), 3617–3625.
Fullerton, H., Rogers, R., Freedman, D.L., Zinder, S.H., 2014. Isolation of an aerobic vinyl chloride oxidizer from anaerobic groundwater. Biodegradation 25 (6), 893–901.
Futamata, H., Nagano, Y., Watanabe, K., Hiraishi, A., 2005. Unique kinetic properties of phenol-degrading variovorax strains responsible for efficient trichloroethylene degradation in a chemostat enrichment culture. Appl. Environ. Microbiol. 71 (2), 904–911. https://doi.org/10.1128/AEM.71.2.904.
Gadkari, J., Goris, T., Schiffmann, C.L., Rubick, R., Adrian, L., Schubert, T., Diekert, G., 2018. Reductive tetrachloroethene dehalogenation in the presence of oxygen by sulfurospirillum multivorans: physiological studies and proteome analysis. FEMS Microbiol. Ecol. 94 (1), fix176.
Gafni, A., Lihl, C., Gelman, F., Elsner, M., Bernstein, A., 2018. δ13C and δ37Cl isotope fractionation to characterize aerobic vs anaerobic degradation of trichloroethylene. Environ. Sci. Technol. Lett. 5 (4), 202–208.
Gafni, A., Gelman, F., Ronen, Z., Bernstein, A., 2020. Variable carbon and chlorine isotope fractionation in TCE co-metabolic oxidation. Chemosphere 242, 125130.
Gaza, S., Schmidt, K.R., Weigold, P., Heidinger, M., Tiehm, A., 2019. Aerobic metabolic trichloroethene biodegradation under field-relevant conditions. Water Res. 151, 343–348.
Goldscheider, N., Hunkeler, D., Rossi, P., 2006. Microbial biocenoses in pristine aquifers and an assessment of investigative methods. Hydrogeol. J. 14 (6), 926–941.
Goren, O., Lazar, B., Burg, A., Gavrieli, I., 2012. Mobilization and retardation of reduced manganese in sandy aquifers: column experiments, modeling and implications. Geochim. Cosmochim. Acta 96, 259–271.
Goris, T., Diekert, G., 2016. The genus Sulfurospirillum. Organohalide-Respiring Bacteria. Springer, Berlin, Heidelberg, pp. 209–234.
Griebler, C., Avramov, M., 2015. Groundwater ecosystem services: a review. Freshw. Sci. 34 (1), 355–367.
Guerrero-Barajas, C., Garcia-Peña, E.I., 2010. Evaluation of enrichments of sulfate reducing bacteria from pristine hydrothermal vents sediments as potential inoculum for reducing trichloroethylene. World J. Microbiol. Biotechnol. 26 (1), 21.
Gupta, A., Widdowson, M.A., 2017. Modeling of complex reductive biodegradation kinetics of recalcitrant organic contaminants. J. Environ. Eng. 143 (8), 04017033.
Hao, L., Zhang, B., Cheng, M., Feng, C., 2016. Effects of various organic carbon sources on simultaneous V (V) reduction and bioelectricity generation in single chamber microbial fuel cells. Bioresour. Technol. 201, 105–110.
Hartwell, J.L., 2000. Survey of Compounds Which Have Been Tested for Carcinogenic Activity (No. 149). Federal Security Agency, US Public Health Service.
He, Y.T., Su, C., 2015. Use of additives in bioremediation of contaminated groundwater and soil. Advances in Bioremediation of Wastewater and Polluted Soilp. 145.
He, J., Ritalahti, K.M., Aiello, M.R., Löffler, F.E., 2003. Complete detoxification of vinyl chloride by an anaerobic enrichment culture and identification of the reductively dechlorinating population as a dehalococcoides species. Appl. Environ. Microbiol. 69 (2), 996–1003.
He, Y.T., Wilson, J.T., Su, C., Wilkin, R.T., 2015. Review of abiotic degradation of chlorinated solvents by reactive iron minerals in aquifers. Groundw. Monit. Remediat. 35 (3), 57–75.
Heidelberg, J.F., Seshadri, R., Haveman, S.A., Hemme, C.L., Paulsen, I.T., Kolonay, J.F., Fraser, C.M., 2004. The genome sequence of the anaerobic, sulfate-reducing bacterium Desulfovibrio vulgaris hildenborough. Nat. Biotechnol. 22 (5), 554–559.
Herrero, J., 2015. Identificació dels processos biogeoquímics que es donen en la zona de la font per al disseny d'estratègies de remediació en aqüífers contaminats per cloroetens (in Catalan). University of Barcelona Doctoral Thewsis.
Herrero, J., Puigserver, D., Nijenhuis, I., Kuntze, K., Carmona, J.M., 2019. Combined use of ISCR and biostimulation techniques in incomplete processes of reductive dehalogenation of chlorinated solvents. Sci. Total Environ. 648, 819–829.
Hu, K., Wang, Q., Tao, G., Wang, A., Ding, D., 2011. Experimental study on restoration of polluted groundwater from in situ leaching uranium mining with sulfate reducing bacteria and ZVI-SRB. Procedia Earth Planet. Sci. 2, 150–155.

Hug, L.A., Maphosa, F., Leys, D., Löffler, F.E., Smidt, H., Edwards, E.A., Adrian, L., 2013. Overview of organohalide-respiring bacteria and a proposal for a classification system for reductive dehalogenases. Philos. Trans. R. Soc. B: Biol. Sci. 368 (1616), 20120322.
Hwang, Y., Shin, H.S., 2013. Effects on nano zero-valent iron reactivity of interactions between hardness, alkalinity, and natural organic matter in reverse osmosis concentrate. J. Environ. Sci. 25 (11), 2177–2184.
Hwang, H.T., Jeen, S.W., Sudicky, E.A., Illman, W.A., 2015. Determination of rate constants and branching ratios for TCE degradation by zero-valent iron using a chain decay multispecies model. J. Contam. Hydrol. 177, 43–53.
Islam, S., Han, Y., Yan, W., 2020. Reactions of chlorinated ethenes with surface-sulfidated iron materials: reactivity enhancement and inhibition effects. Environ. Sci. Process. Impacts 2020 (22), 759–770.
Itoh, T., Yamanoi, K., Kudo, T., et al., 2011. Aciditerrimonas ferrireducens gen. Nov., sp. Nov., an iron-reducing thermoacidophilic actinobacterium isolated from a solfataric field. Int. J. Syst. Evol. Microbiol. 61, 1281–1285. https://doi.org/10.1099/ijs.0.023044-0.
ITRC, 2008. In Situ Bioremediation of Chlorinated Ethene: DNAPL Source Zones. BioDNAPL-3. Interstate Technology & Regulatory Council, Bioremediation of DNAPLs Team, Washington, D.C.
Jeong, H.Y., Hayes, K.F., 2007. Reductive dechlorination of tetrachloroethylene and trichloroethylene by mackinawite (FeS) in the presence of metals: reaction rates. Environ. Sci. Technol. 41 (18), 6390–6396.
Jeong, H.Y., Anantharaman, K., Han, Y.S., Hayes, K.F., 2011. Abiotic reductive dechlorination of cis-dichloroethylene by fe species formed during iron-or sulfate-reduction. Environmental science & technology 45 (12), 5186–5194.
Jørgensen, K.S., 2007. In situ bioremediation. Adv. Appl. Microbiol. 61, 285–305.
Jugder, B.E., Ertan, H., Bohl, S., Lee, M., Marquis, C.P., Manefield, M., 2016. Organohalide respiring bacteria and reductive dehalogenases: key tools in organohalide bioremediation. Front. Microbiol. 7, 249.
Kaiser, J.P., Bollag, J.M., 1990. Microbial activity in the terrestrial subsurface. Experientia 46 (8), 797–806.
Kim, J., Park, W., 2014. Oxidative stress response in pseudomonas putida. Appl. Microbiol. Biotechnol. 98 (16), 6933–6946.
Kim, B.H., Baek, K.H., Cho, D.H., Sung, Y., Koh, S.C., Ahn, C.Y., Kim, H.S., 2010. Complete reductive dechlorination of tetrachloroethene to ethene by anaerobic microbial enrichment culture developed from sediment. Biotechnol. Lett. 32 (12), 1829–1835.
Kim, Y.J., Yang, J.A., Lim, J.K., Park, M.J., Yang, S.H., Lee, H.S., Kwon, K.K., 2020. Paradesulfovibrio onnuriensis gen. nov., sp. nov., a chemolithoautotrophic sulfate-reducing bacterium isolated from the Onnuri vent field of the Indian Ocean and reclassification of Desulfovibrio senegalensis as Paradesulfovibrio senegalensis comb. nov. Journal of Microbiology 1–8.
Koch, H., Lücker, S., Albertsen, M., Kitzinger, K., Herbold, C., Spieck, E., Daims, H., 2015. Expanded metabolic versatility of ubiquitous nitrite-oxidizing bacteria from the genus nitrospira. Proc. Natl. Acad. Sci. 112 (36), 11371–11376.
Kranzioch, I., Stoll, C., Holbach, A., Chen, H., Wang, L., Zheng, B., Tiehm, A., 2013. Dechlorination and organohalide-respiring bacteria dynamics in sediment samples of the Yangtze three gorges reservoir. Environ. Sci. Pollut. Res. 20 (10), 7046–7056.
Kumar, N., Chaurand, P., Rose, J., Diels, L., Bastiaens, L., 2015. Synergistic effects of sulfate reducing bacteria and zero valent iron on zinc removal and stability in aquifer sediment. Chem. Eng. J. 260, 83–89.
Lack, J.G., Chaudhuri, S.K., Chakraborty, R., Achenbach, L.A., Coates, J.D., 2002. Anaerobic biooxidation of fe (II) by dechlorosoma suillum. Microb. Ecol. 424–431.
Lee, J., Lee, T.K., 2016. Development and characterization of PCE-to-ethene dechlorinating microcosms with contaminated river sediment. J. Microbiol. Biotechnol. 26 (1), 120–129.
Leigh, M.B., Wu, W.M., Cardenas, E., Uhlik, O., Carroll, S., Gentry, T., Tiedje, J.M., 2015. Microbial communities biostimulated by ethanol during uranium (VI) bioremediation in contaminated sediment as shown by stable isotope probing. Front. Environ. Sci. Eng. 9 (3), 453–464.
Levar, C.E., Hoffman, C.L., Dunshee, A.J., Toner, B.M., Bond, D.R., 2017. Redox potential as a master variable controlling pathways of metal reduction by geobacter sulfurreducens. ISME J. 11 (3), 741–752.
Li, Y., Li, B., Wang, C.P., Fan, J.Z., Sun, H.W., 2014. Aerobic degradation of trichloroethylene by co-metabolism using phenol and gasoline as growth substrates. Int. J. Mol. Sci. 15 (5), 9134–9148.
Liang, X., Dong, Y., Kuder, T., Krumholz, L.R., Philp, R.P., Butler, E.C., 2007. Distinguishing abiotic and biotic transformation of tetrachloroethylene and trichloroethylene by stable carbon isotope fractionation. Environ. Sci. Technol. 41 (20), 7094–7100.
Liebich, J., Wachtmeister, T., Zhou, J., Burauel, P., 2009. Degradation of diffuse pesticide contaminants: screening for microbial potential using a functional gene microarray. Vadose Zone J. 8 (3), 703–710.
Löffler, F.E., Ritalahti, K.M., Zinder, S.H., 2013. Dehalococcoides and reductive dechlorination of chlorinated solvents. Bioaugmentation for Groundwater Remediation. Springer, New York, NY, pp. 39–88.
Lojkasek-Lima, P., Aravena, R., Shouakar-Stash, O., Frape, S.K., Marchesi, M., Fiorenza, S., Vogan, J., 2012. Evaluating TCE abiotic and biotic degradation pathways in a permeable reactive barrier using compound specific isotope analysis. Groundwater Monit. Remediat. 32 (4), 53–62.
Lonergan, D.J., Jenter, H.L., Coates, J.D., et al., 1996. Phylogenetic analysis of dissimilatory Fe(III)-reducing bacteria. J. Bacteriol. 178, 2402–2408. https://doi.org/10.1128/JB.178.8.2402-2408.1996.
Lookman, R., Bastiaens, L., Borremans, B., Maesen, M., Gemoets, J., Diels, L., 2004. Batch-test study on the dechlorination of 1, 1, 1-trichloroethane in contaminated aquifer material by zero-valent iron. J. Contam. Hydrol. 74 (1–4), 133–144.
Lorah, M.M., Majcher, E.H., Jones, E.J., Voytek, M.A., 2008. Microbial consortia development and microcosm and column experiments for enhanced bioremediation of chlorinated volatile organic compounds. West Branch Canal Creek Wetland Area, Aberdeen Proving Ground, Maryland. U. S. Geological Survey.
Lovley, D., 2006. Dissimilatory Fe (III)-and Mn (IV)-reducing prokaryotes. Prokaryotes 2, 635–658.
Lu, H., Yan, M., Wong, M.H., Mo, W.Y., Wang, Y., Chen, X.W., Wang, J.J., 2020. Effects of biochar on soil microbial community and functional genes of a landfill cover three years after ecological restoration. Sci. Total Environ. 137133.
Luciano, A., Viotti, P., Papini, M.P., 2012. On morphometric properties of DNAPL sources: relating architecture to mass reduction. Water Air Soil Pollut. 223 (5), 2849–2864.
Luo, W., Zhu, X., Chen, W., Duan, Z., Wang, L., Zhou, Y., 2014. Mechanisms and strategies of microbial cometabolism in the degradation of organic compounds–chlorinated ethylenes as the model. Water Sci. Technol. 69 (10), 1971–1983.
Madigan, M.T., Martinko, J.M., Bender, K.S., Buckley, D.H., Stahl, D.A., 2015. Brock Biology of Microorganisms. The United States of America.
Manquián-Cerda, K., Cruces, E., Rubio, M.A., Reyes, C., Arancibia-Miranda, N., 2017. Preparation of nanoscale iron (oxide, oxyhydroxides and zero-valent) particles derived from blueberries: reactivity, characterization and removal mechanism of arsenate. Ecotoxicol. Environ. Saf. 145, 69–77.
Mattes, A., Gould, D., Taupp, M., Glasauer, S., 2013. A novel autotrophic bacterium isolated from an engineered wetland system links nitrate-coupled iron oxidation to the removal of as, zn and S. Water Air Soil Pollut. 224 (4), 1490.
Mattes, T.E., Jin, Y.O., Livermore, J., Pearl, M., Liu, X., 2015. Abundance and activity of vinyl chloride (VC)-oxidizing bacteria in a dilute groundwater VC plume biostimulated with oxygen and ethene. Appl. Microbiol. Biotechnol. 99 (21), 9267–9276.
McCarty, P.L., 2016. Discovery of organohalide-respiring processes and the bacteria involved. Organohalide-Respiring Bacteria. Springer, Berlin, Heidelberg, pp. 51–62.
McMahon, P.B., Chapelle, F.H., 2008. Redox processes and water quality of selected principal aquifer systems. Groundwater 46 (2), 259–271.
McMahon, P.B., Chapelle, F.H., Bradley, P.M., 2011. Evolution of redox processes in groundwater. Aquatic Redox Chemistry. American Chemical Society, pp. 581–597.
Mehta, D., Satyanarayana, T., 2013. Diversity of hot environments and thermophilic microbes. Thermophilic Microbes in Environmental and Industrial Biotechnology. Springer, Dordrecht, pp. 3–60.
Mehta-Kolte, M.G., Bond, D.R., 2012. Geothrix fermentans secretes two different redox-active compounds to utilize electron acceptors across a wide range of redox potentials. Appl. Environ. Microbiol. 78 (19), 6987–6995.
Menon, P., Voordouw, G., 2018. Impact of light oil toxicity on sulfide production by acetate-oxidizing, sulfate-reducing bacteria. Int. Biodeterior. Biodegradation 126, 208–215.
Miao, Z., Brusseau, M.L., Carroll, K.C., Carreón-Diazconti, C., Johnson, B., 2012. Sulfate reduction in groundwater: characterization and applications for remediation. Environ. Geochem. Health 34 (4), 539–550.
Mohaupt, V., Crosnier, G., Todd, R., Petersen, P., Dworak, T., 2007. WFD and agriculture activity of the EU: first linkages between the CAP and the WFD at EU level. Water Sci. Technol. 56 (1), 163–170.
Moons, P., Michiels, C.W., Aertsen, A., 2009. Bacterial interactions in biofilms. Crit. Rev. Microbiol. 35 (3), 157–168.
Němeček, J., Dolinová, I., Macháčková, J., Špánek, R., Ševců, A., Lederer, T., Černík, M., 2017. Stratification of chlorinated ethenes natural attenuation in an alluvial aquifer assessed by hydrochemical and biomolecular tools. Chemosphere 184, 1157–1167.
Němeček, J., Marková, K., Špánek, R., Antoš, V., Kozubek, P., Lhotský, O., Černík, M., 2020. Hydrochemical conditions for Aerobic/Anaerobic biodegradation of chlorinated Ethenes—A multi-site assessment. Water 12 (2), 322.
Nestler, H., Kiesel, B., Kaschabek, S.R., Mau, M., Schlömann, M., Balcke, G.U., 2007. Biodegradation of chlorobenzene under hypoxic and mixed hypoxic-denitrifying conditions. Biodegradation 18 (6), 755–767.
Nevin, K.P., Lovley, D.R., 2002. Mechanisms for accessing insoluble fe (III) oxide during dissimilatory fe (III) reduction by geothrix fermentans. Appl. Environ. Microbiol. 68 (5), 2294–2299.
Newell, C.J., Kueper, B.H., Wilson, J.T., Johnson, P.C., 2014. Natural attenuation of chlorinated solvent source zones. Chlorinated Solvent Source Zone Remediation. Springer, New York, NY, pp. 459–508.
Nijenhuis, I., Kuntze, K., 2016. Anaerobic microbial dehalogenation of organohalides-state of the art and remediation strategies. Curr. Opin. Biotechnol. 38, 33–38.
Oldham, V.E., Jones, M.R., Tebo, B.M., Luther III, G.W., 2017. Oxidative and reductive processes contributing to manganese cycling at oxic-anoxic interfaces. Mar. Chem. 195, 122–128.
Pan, Y., Yang, X., Xu, M., Sun, G., 2017. The role of enriched microbial consortium on iron-reducing bioaugmentation in sediments. Front. Microbiol. 8, 462.
Pankow, J.F., Cherry, J.A., 1996. Dense Chlorinated Solvents and Other DNAPLs in Groundwater: History, Behavior, and Remediation. Waterloo Press, Ontario.
Pant, P., Pant, S., 2010. A review: advances in microbial remediation of trichloroethylene (TCE). J. Environ. Sci. 22 (1), 116–126.
Parker, B.L., Cherry, J.A., Chapman, S.W., Guilbeault, M.A., 2003. Review and analysis of chlorinated solvent dense nonaqueous phase liquid distributions in five sandy aquifers. Vadose Zone J. 2 (2), 116–137.
Paszczynski, A.J., Paidisetti, R., Johnson, A.K., Crawford, R.L., Colwell, F.S., Green, T., Conrad, M., 2011. Proteomic and targeted qPCR analyses of subsurface microbial communities for presence of methane monooxygenase. Biodegradation 22 (6), 1045–1059.
Patil, S.S., Adetutu, E.M., Ball, A.S., 2014. Microbiology of chloroethene degradation in groundwater. Microbiol. Aust. 35 (4), 211–214.
Patterson, B.M., Lee, M., Bastow, T.P., Wilson, J.T., Donn, M.J., Furness, A., Manefield, M., 2016. Concentration effects on biotic and abiotic processes in the removal of 1, 1, 2-trichloroethane and vinyl chloride using carbon-amended ZVI. J. Contam. Hydrol. 188, 1–11.
Paul, L., Jakobsen, R., Smolders, E., Albrechtsen, H.J., Bjerg, P.L., 2016. Reductive dechlorination of trichloroethylene (TCE) in competition with fe and mn oxides—observed dynamics in H2-dependent terminal electron accepting processes. Geomicrobiol J. 33 (5), 357–366.
Peng, Y.H., Shih, Y.H., 2013. Microbial degradation of some halogenated compounds: Biochemical and molecular features. In: Chamy, R., Rosenkranz, F. (Eds.), Biodegradation of Hazardous and Special Products, pp. 51–69.

Petrangeli, M.P., Majone, M., Arjmand, F., Silvestri, D., Sagliaschi, M., Sucato, S., Alesi, E., 2016. First pilot test on the integration of GCW (groundwater circulation well) with ENA (enhanced natural attenuation) for chlorinated solvents source remediation. Chem. Eng. Trans. 49, 91–96.
Phenrat, T., Le, T.S.T., Naknakorn, B., Lowry, G.V., 2019. Chemical reduction and oxidation of organic contaminants by nanoscale zerovalent iron. Nanoscale Zerovalent Iron Particles for Environmental Restoration. Springer, Cham, pp. 97–155.
Puigserver, D., Carmona, J.M., Barker, J., Cortes, A., Nogueras, X., Viladevall, M., 2011. Use of chemical and biological techniques in the remediation of sites contaminated by chlorinated solvents. Journal of IAHS-AISH. International Association of Hydrological Sciences 445–448.
Puigserver, D., Carmona, J.M., Cortés, A., Viladevall, M., Nieto, J.M., Grifoll, M., Parker, B.L., 2013. Subsoil heterogeneities controlling porewater contaminant mass and microbial diversity at a site with a complex pollution history. J. Contam. Hydrol. 144 (1), 1–19.
Puigserver, D., Cortés, A., Viladevall, M., Nogueras, X., Parker, B.L., Carmona, J.M., 2014. Processes controlling the fate of chloroethenes emanating from DNAPL aged sources in river–aquifer contexts. J. Contam. Hydrol. 168, 25–40.
Puigserver, D., Herrero, J., Torres, M., Cortés, A., Nijenhuis, I., Kuntze, K., Carmona, J.M., 2016. Reductive dechlorination in recalcitrant sources of chloroethenes in the transition zone between aquifers and aquitards. Environ. Sci. Pollut. Res. 23 (18), 18724–18741.
Puigserver, D., Herrero, J., Parker, B.L., Carmona, J.M., 2020. Natural attenuation of pools and plumes of carbon tetrachloride and chloroform in the transition zone to bottom aquitards and the microorganisms involved in their degradation. Sci. Total Environ. 712, 135679.
Puigserver, D., Herrero, J., Nogueras, X., Cortés, A., Parker, B.L., Playà, E., Carmona, J.M., 2022. Biotic and abiotic reductive dechlorination of chloroethenes in aquitards. Sci. Total Environ. 816, 151532.
Rahm, B.G., Chauhan, S., Holmes, V.F., Macbeth, T.W., Kent Jr., S., Alvarez-Cohen, L., 2006. Molecular characterization of microbial populations at two sites with differing reductive dechlorination abilities. Biodegradation 17 (6), 523–534.
Rajajayavel, S.R.C., Ghoshal, S., 2015. Enhanced reductive dechlorination of trichloroethylene by sulfidated nanoscale zerovalent iron. Water Res. 78, 144–153.
Reinsch, B.C., Forsberg, B., Penn, R.L., Kim, C.S., Lowry, G.V., 2010. Chemical transformations during aging of zerovalent iron nanoparticles in the presence of common groundwater dissolved constituents. Environ. Sci. Technol. 44 (9), 3455–3461.
Rivett, M.O., Dearden, R.A., Wealthall, G.P., 2014. Architecture, persistence and dissolution of a 20 to 45 year old trichloroethene DNAPL source zone. J. Contam. Hydrol. 170, 95–115.
Robinson, C., Barry, D.A., 2009. Design tool for estimation of buffer requirement for enhanced reductive dechlorination of chlorinated solvents in groundwater. Environ. Model Softw. 24 (11), 1332–1338.
Rossi, P., Shani, N., Kohler, F., Imfeld, G., Holliger, C., 2012. Ecology and biogeography of bacterial communities associated with chloroethene-contaminated aquifers. Front. Microbiol. 3, 260.
Saiyari, D.M., Chuang, H.P., Senoro, D.B., Lin, T.F., Whang, L.M., Chiu, Y.T., Chen, Y.H., 2018. A review in the current developments of genus dehalococcoides, its consortia and kinetics for bioremediation options of contaminated groundwater. Sustain. Environ. Res. 28 (4), 149–157.
Schaefer, C.E., Lavorgna, G.M., Haluska, A.A., Annable, M.D., 2018. Long-term impacts on groundwater and reductive dechlorination following bioremediation in a highly characterized trichloroethene DNAPL source area. Groundw. Monit. Remediat. 38 (3), 65–74.
Schiwy, A., Maes, H.M., Koske, D., Flecken, M., Schmidt, K.R., Schell, H., Heggen, M., 2016. The ecotoxic potential of a new zero-valent iron nanomaterial, designed for the elimination of halogenated pollutants, and its effect on reductive dechlorinating microbial communities. Environ. Pollut. 216, 419–427.
Schmidt, T.C., Jochmann, M.A., 2012. Origin and fate of organic compounds in water: characterization by compound-specific stable isotope analysis. Annu. Rev. Anal. Chem. 5, 133–155.
Schmidt, K.R., Augenstein, T., Heidinger, M., Ertl, S., Tiehm, A., 2010. Aerobic biodegradation of cis-1, 2-dichloroethene as sole carbon source: stable carbon isotope fractionation and growth characteristics. Chemosphere 78 (5), 527–532.
Schmidt, K.R., Gaza, S., Voropaev, A., Ertl, S., Tiehm, A., 2014. Aerobic biodegradation of trichloroethene without auxiliary substrates. Water Res. 59, 112–118.
Sekhohola-Dlamini, L., Tekere, M., 2019. Microbiology of municipal solid waste landfills: a review of microbial dynamics and ecological influences in waste bioprocessing. Biodegradation 1–21.
Shirokova, V.L., Ferris, F.G., 2013. Microbial diversity and biogeochemistry of a shallow pristine Canadian shield groundwater system. Geomicrobiol J. 30 (2), 140–149.
Slater, G.F., Sherwood Lollar, B., Sleep, B.E., Edwards, E.A., 2001. Variability in carbon isotopic fractionation during biodegradation of chlorinated ethenes: implications for field applications. Environ. Sci. Technol. 35 (5), 901–907.
Smith, G.J., Wang, Y., 2010. Groundwater geochemistry diagnostics during in situ ERH remediation. Remediat. J. 21 (1), 97–114.
Song, D.L., Conrad, M.E., Sorenson, K.S., Alvarez-Cohen, L., 2002. Stable carbon isotope fractionation during enhanced in situ bioremediation of trichloroethene. Environ. Sci. Technol. 36 (10), 2262–2268.
Sonthiphand, P., Hall, M.W., Neufeld, J.D., 2014. Biogeography of anaerobic ammonia-oxidizing (anammox) bacteria. Front. Microbiol. 5, 399.
Starke, R., Müller, M., Gaspar, M., Marz, M., Küsel, K., Totsche, K.U., Jehmlich, N., 2017. Candidate brocadiales dominates C, N and S cycling in anoxic groundwater of a pristine limestone-fracture aquifer. J. Proteome 152, 153–160.
Stefaniuk, M., Oleszczuk, P., Ok, Y.S., 2016. Review on nano zerovalent iron (nZVI): from synthesis to environmental applications. Chem. Eng. J. 287, 618–632.
Straub, K.L., Schonhuber, W.A., Buchholz-Cleven, B.E.E., Schink, B., 2004. Diversity of ferrous iron-oxidizing, nitrate-reducing bacteria and their involvement in oxygen-independent iron cycling. Geomicrobiol J. 21, 371–378.
Stroo, H.F., West, M.R., Kueper, B.H., Borden, R.C., Major, D.W., Ward, C.H., 2014. In situ bioremediation of chlorinated ethene source zones. Chlorinated Solvent Source Zone Remediation. Springer, New York, NY, pp. 395–457.
Sun, Y., Li, J., Huang, T., Guan, X., 2016. The influences of iron characteristics, operating conditions and solution chemistry on contaminants removal by zero-valent iron: a review. Water Res. 100, 277–295.
Tabernacka, A., Zborowska, E., Pogoda, K., Żołądek, M., 2019. Removal of tetrachloroethene from polluted air by activated sludge. Environ. Technol. 40 (4), 470–479.
Tesoriero, A.J., Liebscher, H., Cox, S.E., 2000. Mechanism and rate of denitrification in an agricultural watershed: electron and mass balance along groundwater flow paths. Water Resour. Res. 36 (6), 1545–1559.
Thornton, S.F., Morgan, P., Rolfe, S.A., 2016. Bioremediation of hydrocarbons and chlorinated solvents in groundwater: Characterisation, design and performance assessment. Hydrocarbon and Lipid Microbiology Protocols. Springer, Berlin, Heidelberg, pp. 11–64.
Tiehm, A., Schmidt, K.R., 2011. Sequential anaerobic/aerobic biodegradation of chloroethenes-aspects of field application. Curr. Opin. Biotechnol. 22 (3), 415–421.
Tobiszewski, M., Namieśnik, J., 2012. Abiotic degradation of chlorinated ethanes and ethenes in water. Environ. Sci. Pollut. Res. 19 (6), 1994–2006.
Van Breukelen, B.M., Hunkeler, D., Volkering, F., 2005. Quantification of sequential chlorinated ethene degradation by use of a reactive transport model incorporating isotope fractionation. Environ. Sci. Technol. 39 (11), 4189–4197.
Van Hullebusch, E.D., Huguenot, D., Pechaud, Y., Simonnot, M.O., Colombano, S. (Eds.), 2020. Environmental Soil Remediation and Rehabilitation: Existing and Innovative Solutions. Springer International Publishing.
Weatherill, J.J., Krause, S., Ullah, S., Cassidy, N.J., Levy, A., Drijfhout, F.P., Rivett, M.O., 2019. Revealing chlorinated ethene transformation hotspots in a nitrate-impacted hyporheic zone. Water Res. 161, 222–231.
Wei, N., Finneran, K.T., 2011. Influence of ferric iron on complete dechlorination of trichloroethylene (TCE) to ethene: Fe (III) reduction does not always inhibit complete dechlorination. Environ. Sci. Technol. 45 (17), 7422–7430.
Wei, X., Rodak, C.M., Zhang, S., Han, Y., Wolfe, F.A., 2016. Mine drainage generation and control options. Water Environ. Res. 88 (10), 1409–1432.
Wei, Y.T., Wu, S.C., Yang, S.W., Che, C.H., Lien, H.L., Huang, D.H., 2012. Biodegradable surfactant stabilized nanoscale zero-valent iron for in situ treatment of vinyl chloride and 1, 2-dichloroethane. J. Hazard. Mater. 211, 373–380.
Wen, L.L., Zhang, Y., Pan, Y.W., Wu, W.Q., Meng, S.H., Zhou, C., Zhao, H.P., 2015. The roles of methanogens and acetogens in dechlorination of trichloroethene using different electron donors. Environ. Sci. Pollut. Res. 22 (23), 19039–19047.
Wiegert, C., Mandalakis, M., Knowles, T., Polymenakou, P.N., Aeppli, C., Macháčková, J., Gustafsson, O., 2013. Carbon and chlorine isotope fractionation during microbial degradation of tetra-and trichloroethene. Environ. Sci. Technol. 47 (12), 6449–6456.
Wilson, F.P., Liu, X., Mattes, T.E., Cupples, A.M., 2016. Nocardioides, sediminibacterium, aquabacterium, variovorax, and pseudomonas linked to carbon uptake during aerobic vinyl chloride biodegradation. Environ. Sci. Pollut. Res. 23 (19), 19062–19070.
Wu, N., Zhang, W., Wei, W., Yang, S., Wang, H., Sun, Z., Yang, Y., 2020. Field study of chlorinated aliphatic hydrocarbon degradation in contaminated groundwater via micron zero-valent iron coupled with biostimulation. Chem. Eng. J. 384, 123349.
Xie, Y., Cwiertny, D.M., 2012. Influence of anionic cosolutes and pH on nanoscale zerovalent iron longevity: time scales and mechanisms of reactivity loss toward 1, 1, 1, 2-tetrachloroethane and Cr (VI). Environ. Sci. Technol. 46 (15), 8365–8373.
Xin, X., Chen, B.Y., Hong, J., 2019. Unraveling interactive characteristics of microbial community associated with bioelectric energy production in sludge fermentation fluid-fed microbial fuel cells. Bioresour. Technol. 289, 121652.
Xu, X.J., Chen, C., Guan, X., Yuan, Y., Wang, A.J., Lee, D.J., Ren, N.Q., 2017. Performance and microbial community analysis of a microaerophilic sulfate and nitrate co-reduction system. Chem. Eng. J. 330, 63–70.
Xu, H., Tong, N., Huang, S., Hayat, W., Fazal, S., Li, J., Zhang, Y., 2018. Simultaneous autotrophic removal of sulphate and nitrate at different voltages in a bioelectrochemical reactor (BER): evaluation of degradation efficiency and characterization of microbial communities. Bioresour. Technol. 265, 340–348.
Yang, Y., McCarty, P.L., 2000. Biologically enhanced dissolution of tetrachloroethene DNAPL. Environ. Sci. Technol. 34, 2979–2984.
Yang, Y., McCarty, P.L., 2002. Comparison between donor substrates for biologically enhanced tetrachloroethene DNAPL dissolution. Environ. Sci. Technol. 36, 3400–3404.
Yang, J., Meng, L., Guo, L., 2018. In situ remediation of chlorinated solvent-contaminated groundwater using ZVI/organic carbon amendment in China: field pilot test and full-scale application. Environ. Sci. Pollut. Res. 25 (6), 5051–5062.
Yang, C.E., Wu, C.Y., Liu, Y.C., Lan, E.I., Tsai, S.L., 2019. Cometabolic degradation of toluene and TCE contaminated wastewater in a bench-scale sequencing batch reactor inoculated with immobilized pseudomonas putida F1. J. Taiwan Inst. Chem. Eng. 104, 168–176.
Yu, S., Lee, P.K., Hwang, S.I., 2015. Groundwater contamination with volatile organic compounds in urban and industrial areas: analysis of co-occurrence and land use effects. Environ. Earth Sci. 74 (4), 3661–3677.
Zeng, D., Yin, Q., Du, Q., Wu, G., 2019. System performance and microbial community in ethanol-fed anaerobic reactors acclimated with different organic carbon to sulfate ratios. Bioresour. Technol. 278, 34–42.
Zhang, S., Hou, Z., Du, X.M., Li, D.M., Lu, X.X., 2016. Assessment of biostimulation and bioaugmentation for removing chlorinated volatile organic compounds from groundwater at a former manufacture plant. Biodegradation 27 (4–6), 223–236.
Zhang, L., Zeng, Q., Liu, X., Chen, P., Guo, X., Ma, L.Z., Huang, Y., 2019. Iron reduction by diverse actinobacteria under oxic and pH-neutral conditions and the formation of secondary minerals. Chem. Geol. 525, 390–399.
Zhou, A.X., Zhang, Y.L., Dong, T.Z., Lin, X.Y., Su, X.S., 2015. Response of the microbial community to seasonal groundwater level fluctuations in petroleum hydrocarbon-contaminated groundwater. Environ. Sci. Pollut. Res. 22 (13), 10094–10106.
Zinder, S.H., 2016. The genus dehalococcoides. Organohalide-Respiring Bacteria. Springer, Berlin, Heidelberg, pp. 107–136.